Effects of a sublethal and transient stress of the endoplasmic reticulum on the mitochondrial population

Vannuvel, Kayleen; Van Steenbrugge, Martine; Demazy, Catherine; Ninane, Noëlle; Fattaccioli, Antoine; Fransolet, Maude; Renard, Patricia; Raes, Martine; Arnould, Thierry

Published in:
Journal of Cellular Physiology

DOI:
10.1002/jcp.25292

Publication date:
2016

Journal of Cellular Physiology

Effects of a Sublethal and Transient Stress of the Endoplasmic Reticulum on the Mitochondrial Population

KAYLEEN VANNUVEL, MARTINE VAN STEENBRUGGE, CATHERINE DEMAZY, NOËLLE NINANE, ANTOINE FATTACCIOLI, MAUDE FRANSOLET, PATRICIA RENARD, MARTINE RAES, AND THIERRY ARNOULD*

Laboratory of Biochemistry and Cell Biology (URBC), Namur Research Institute for Life Sciences (NARILIS), University of Namur (UNamur), Namur, Belgium

Endoplasmic reticulum (ER) and mitochondria are not discrete intracellular organelles but establish close physical and functional interactions involved in several biological processes including mitochondrial bioenergetics, calcium homeostasis, lipid synthesis, and the regulation of apoptotic cell death pathways. As many cell types might face a transient and sublethal ER stress during their lifetime, it is thus likely that the adaptive UPR response might affect the mitochondrial population. The aim of this work was to study the putative effects of a non-lethal and transient endoplasmic reticulum stress on the mitochondrial population in HepG2 cells. The results show that thapsigargin and brefeldin A, used to induce a transient and sublethal ER stress, rapidly lead to the fragmentation of the mitochondrial network associated with a decrease in mitochondrial membrane potential, $O_2^{\bullet -}$ production and less efficient respiration. These changes in mitochondrial function are transient and preceded by the phosphorylation of JNK. Inhibition of JNK activation by SP600125 prevents the decrease in $O_2^{\bullet -}$ production and the mitochondrial network fragmentation observed in cells exposed to the ER stress but has no impact on the reduction of the mitochondrial membrane potential. In conclusion, our data show that a non-lethal and transient ER stress triggers a rapid activation of JNK without inducing apoptosis, leading to the fragmentation of the mitochondrial network and a reduction of $O_2^{\bullet -}$ production.

J. Cell. Physiol. 231: 1913–1931, 2016.

The endoplasmic reticulum (ER) is a multifunctional organelle that participates in various biosynthetic and signaling pathways, of which the primary function is synthesis, folding, and quality control of the proteins of the secretory pathway (Berridge, 2002; Groenendyk and Michalak, 2005). The ER is also the major site of Ca^{2+} storage in the cell and plays an important role in the synthesis of cholesterol, steroids, and various lipids contributing to various cell membrane structures (Baumann and Walz, 2001; Fu et al., 2012). ER homeostasis is thus essential to maintain cell function and survival and cells are extremely sensitive to physiological conditions that disturb the normal ER environment or demand an increase in protein synthesis, maturation, and folding in the secretory pathway (Dufey et al., 2014; Lee and Ozcan, 2014). For example, a physiological ER stress occurs in a variety of normal cellular processes, such as the differentiation of B lymphocyte (Gass et al., 2002; Cenci and Sitia, 2007), lipid metabolism in the liver (Zheng et al., 2010; Wang and Kaufman, 2014), or in pancreatic β-cells involved in high-rate insulin synthesis (Papa, 2012; Sun et al., 2015).

ER stress related to accumulation of unfolded proteins is defined as a cellular state in which the capacity of the ER is overwhelmed by a protein overload and/or a disruption of its folding capacity (Hetz, 2012; Urra et al., 2013). Many physiological and/or environmental perturbations including accumulation of misfolded and aggregated proteins (Benyair et al., 2011; Snapp, 2012), redox changes (Delic et al., 2012; Landau et al., 2013), alterations in Ca^{2+} homeostasis (Sammels et al., 2010), glucose deprivation (Iwawaki and Oikawa, 2013; de la Cadena et al., 2014) or viral infection (Pineau et al., 2009) are known to trigger the activation of a conserved adaptive signaling pathway, called the er-unfolded protein response (UPR^{er}). This response involves signaling pathways activated by transmembrane sensors at the luminal face of ER membrane and initiation of a transduction cascade in attempt to restore

Abbreviations: ATF6, activating transcription factor 6; BFA, brefeldin A; Ca^{2+}, calcium; Drp1, dynamin related protein 1; ECAR, extracellular acidification rate; ER, endoplasmic reticulum; FCCP, carbonyl cyanide p trifluoromethoxyphenylhydrazone; Fis1, fission 1; HADHA, hydroxyacyl CoA dehydrogenase/3-ketoacyl-CoA thiolase/enoyl-CoA hydratase; IMM, inner mitochondrial membrane; IRE 1, inositol-requiring enzyme 1; JNK, c Jun N-terminal kinase; MAM, mitochondria associated membranes; Mff, mitochondrial fission factor; Mfn1, mitofusin 1; Mfn2, mitofusin 2; MiD49, mitochondrial dynamics protein of 49 kDa; MiD51, mitochondrial dynamics protein of 51 kDa; MPTP, mitochondrial permeability transition pore; OCR, oxygen consumption rate; OMM, outer mitochondrial membrane; Opa1, optic atrophy factor 1; PERK, protein kinase RNA like endoplasmic reticulum kinase; ROS, reactive oxygen species; SOD2, superoxide dismutase 2; TG, thapsigargin; UPR, unfolded protein response; XBP 1, X-box binding protein 1.

Contract grant sponsor: Belgian Association for Muscular Diseases;
Contract grant number: 2013-08.
Contract grant sponsor: University of Namur.
Contract grant sponsor: Fonds de la Recherche Scientifique;
Contract grant number: 2.5008.11.

*Correspondence to: Thierry Arnould, Laboratory of Biochemistry and Cell Biology (URBC), Namur Research Institute for LIfe Sciences (NARILIS), University of Namur (UNamur), 61 rue de Bruxelles, Namur 5000, Belgium. E-mail: thierry.arnould@unamur.be

Manuscript Received: 22 April 2015
Manuscript Accepted: 15 December 2015

Accepted manuscript online in Wiley Online Library (wileyonlinelibrary.com): 17 December 2015.
DOI: 10.1002/jcp.25292

cellular homeostasis (Walter and Ron, 2011). Three ER-resident transmembrane proteins have been identified as sensors of ER stress that initiate the UPR^{er}:PERK (protein kinase RNA-like endoplasmic reticulum kinase), IRE1 (inositol-requiring kinase I), and ATF6 (activating transcription factor 6) (for comprehensive and recent reviews see (Wakabayashi and Yoshida, 2013; Brewer, 2014)). These sensors are usually maintained in an inactive state by a major ER chaperone, BiP (immunoglobulin heavy chain-binding protein)/Grp78 (Hamman et al., 1998). Under conditions of ER stress, BiP is released from the ER sensors, allowing activation of the UPR (Bertolotti et al., 2000). Both IRE1 and PERK homodimerize upon release of BiP and undergo autophosphorylation, leading to the production of active transcription factors, XBP-1, and ATF4, respectively (Ma et al., 2002; Li et al., 2010). In addition, ATF6 is transported to the Golgi where it is cleaved proteolytically into an active transcription factor (Shen and Prywes, 2004). XBP-1, AT4, and ATF6, in turn, activate downstream target genes to restore ER homeostasis. Depending on the severity and the duration of the stress, and especially when homeostasis cannot be restored, the UPR switches to induce cell death caused by either mitochondria-dependent or -independent apoptosis (Urra et al., 2013; Vannuvel et al., 2013). Mitochondria are essential organelles for ATP production by oxidative phosphorylation, for the synthesis of many important metabolites (amino acids, steroids, phospholipids, ...), the participation to the β-oxidation of free fatty acids and the regulation of calcium homeostasis (Duchen, 2004). Besides their role in cell metabolism and survival, it is now well demonstrated that mitochondria play a key role in the integration of cell death signals (Regula et al., 2003; Bras et al., 2005).

Over the past few decade, the traditional view of the ER and mitochondria as individual, separate and independent entities has profoundly changed and it is now evident that both, the ER and mitochondria, are highly dynamic interconnected organelles that undergo continuous spatial and structural reorganization affecting organelle functions (Lackner, 2014; Westrate et al., 2015). Indeed, recent studies demonstrated that organelle morphological changes have an effect on function and could be involved in several pathologies such as type 2 diabetes, neurodegenerative disorders, and cardiovascular diseases (Galloway and Yoon, 2013; Burte et al., 2015; Iqbal and Hood, 2015; Kucharz et al., 2013).

More specifically, both organelles establish physical tight contacts throughout their networks, called the mitochondria-associated membranes (MAMs), involved in Ca^{2+} exchange and in the transfer of metabolites including lipids, regulating biological functions, such as lipid homeostasis, mitochondrial metabolism, and apoptotic signaling (Marchi et al., 2014; Vance, 2014). Thus, the ER-mitochondria contacts build up a platform orchestrating inter-organelle communication that is important for the coordination of cellular functions. In fact, it is now established that ER wraps around mitochondria and mediates mitochondrial division at contact sites controlling mitochondrial dynamics (Friedman et al., 2011; Ohta et al., 2014). Given the importance of these close interactions, a stress induced in the ER could have an impact on the biology of mitochondria allowing prosurvival adaptations or initiation of a proapoptotic response, depending on the duration and/or intensity of the ER stress. Although, so far, the vast majority of the studies in the field were focused on chronic and severe ER stress shown to trigger mitochondria-dependent apoptosis (Hom et al., 2007; Baumgartner et al., 2009; Yen et al., 2012), recently, Bravo and co-workers demonstrated that, during the early adaptive phase of a sustained severe ER stress, the number of ER-mitochondria contact points increases whereas both networks are re-localized toward the perinuclear area (Bravo et al., 2011). These authors also suggest that increasing ER-mitochondria connections promote Ca^{2+} release from the ER to mitochondria, a process known to stimulate mitochondrial metabolism by the activation of Ca^{2+}-regulated dehydrogenases involved in the tricarboxylic acid (TCA) cycle. The bioenergetic capacity of the cell would thus be improved, as well as the energetic resources contributing favorably to the cellular adaptation to ER stress (Bravo et al., 2011).

However, the putative mechanisms involved in the maintenance of cell survival during a mild non-lethal and transient ER stress are not yet fully understood. In this study, the effects of a mild and transient ER stress on mitochondrial bioenergetics and dynamics were analyzed in a model of cultured human hepatoma cells. More precisely, we used two well-known ER stress inducers: thapsigargin (TG), an inhibitor of the SERCA pumps, inhibiting the entry of calcium in the ER lumen leading to ER stress due to a depletion of calcium (Lytton et al., 1991) and brefeldin A (BFA), an inhibitor of the transport of proteins from the ER to the Golgi apparatus causing an accumulation of proteins within the ER (Fujiwara et al., 1988; Slomiany et al., 1993). We provide evidence that a mild-ER stress induced by these agents, activates the UPR without triggering apoptosis. We also show that a non-lethal stress provokes fragmentation of the mitochondrial network accompanied with a decrease in the mitochondrial membrane potential, mitochondrial $O_2^{\bullet -}$ production and respiration, suggesting an adaptation of the cell to the applied stress. These changes are reversible as a recovery of mitochondrial functions back to normal is observed after a resting period during which cells are no longer exposed to the ER stress. Finally, the mitochondrial network fragmentation and reduction of $O_2^{\bullet -}$ production in response to the ER stress might be dependent on the rapid and transient activation of JNK, as the inhibition of this Ser/Thr kinase prevents these changes without affecting the ER stress-induced reduction of the mitochondrial membrane potential.

Materials and Methods

Cell culture and reagents

Human hepatoma cells (HepG2 cells) were cultured in Dulbecco's modified Eagle's medium (DMEM, Gibco, Life Technologies, Carlsbad, CA) supplemented with 10% of FBS (fetal bovine serum) in a 5% CO_2 humidified 37°C incubator. At 70% confluence, cells were trypsinized and subcultured in 24-, 12-, and 6-well culture plates or 25 or 75 cm^2 culture flasks, according to the experimental or maintainance needs of cell culture (Corning, Inc., New York, NY).

Cells were seeded and 24 h later, ER stress was induced with 50 nM thapsigargin (TG, Sigma–Aldrich, Saint-Louis, MO) or 500 nM brefeldin A (BFA, B7651, Sigma–Aldrich) for the indicated incubation times. In some experiments, to allow a recovery period, cells were first pre-incubated with TG or BFA for 6 or 10 h before replacing the media by complete fresh medium. JNK phosphorylation inhibition was performed by pre-incubating cells for 1 h with 40 μM SP600125 (Tocris Bioscience, Bristol, UK).

LDH release

TG and BFA toxicity was assessed by monitoring LDH release using a Cytotoxicity Detection kit (Roche Molecular Biochemical, Basel, Switzerland) according to the manufacturer's protocol. The day prior to the assay, HepG2 cells were seeded in 12-well culture plates (Corning) at a density of 75,000 cells per well. The cells were incubated with different concentrations of TG or BFA for 6 or 10 h, respectively (chosen as the maximum incubation times that do not display cell death markers, data not shown). At the end of the incubations, fresh complete medium + 10% FBS was added for 42 or 38 h for TG- or BFA-treated cells, respectively. The culture media from incubated cells were centrifuged (Centrifuge 5415R 5, Eppendorf, Hamburg, Germany) for 5 min at 2,000 rpm to pellet the cell fragments and apoptotic bodies. Adhering and pelleted cells

were then lysed in PBS containing 10% Triton X-100 (Sigma–Aldrich). A positive control was used by incubating cells with 50 μM etoposide for 16 h followed by a recovery period of 32 h. The percentages of LDH release were calculated as: LDH activity in media (1) + LDH activity in pelleted cells (2)/(1) + (2) + LDH activity of remaining adhering cells in the wells. Results are presented in percentages of release as means ± SD for three independent experiments (n = 3).

Western blotting analysis

The abundance of proteins and their modified form was analyzed using fluorescence-based Western blot detection (Li-Cor Biosciences, Lincoln, NE) (Gingrich et al., 2000; Lewis et al., 2003). HepG2 cells were seeded at a density of 1.10^6 cells in 25 cm^2 culture flasks and the next day, cells were incubated in the presence of 50 nM TG or 500 nM BFA. Total cell lysates were prepared in DLA (Dye Labeling Amino acid) buffer (7 M urea, 2 M thiourea, 4% CHAPS, 30 mM Tris; pH 7.4) supplemented with Complete Protease Inhibitor Cocktail (Roche, Basel, Switzerland) and 4% phosphatase inhibitor cocktail (25 mM Na_3VO_4, 250 mM 4-nitrophenylphosphate, 250 mM glycerophosphate, 125 mM NaF). Protein concentration was determined using the 660 nm Pierce assay kit (Thermo Fisher Scientific, Waltham, MA). An amount of 15 μg of total cell lysates were resolved by gel electrophoresis using 4–12% Bis-Tris precast gels (Novex, Life Technologies). The proteins were then electrotransferred (semi-dry device) for 2 h onto PVDF (PolyVinylDieneFluoride, Amersham, GE Healthcare Europe, GmbHDiegem, Belgium) membranes (Merck Millipore, Bellerica, MA). Unspecific binding sites were blocked by incubating the membranes for 1 h at room temperature with blocking solution (Li-Cor Odyssey Infrared Imaging System blocking buffer diluted twice in PBS). Western blot analysis was performed using the primary antibodies listed in Table 1, secondary antibodies coupled to Infrared dyes (1:7500, Li-Cor Biosciences) and by detecting infrared fluorescence (Odyssey scanner, Li-Cor Biosciences). The fluorescence intensity of the bands corresponding to the protein of interest was quantified using the Odyssey V3.0 application software (Li-Cor Biosciences) and normalized by the fluorescence intensity of the bands corresponding to the immunodetection of α-tubulin or β-actin used as loading control.

Transient transfection and luciferase assay

HepG2 cells were transiently co-transfected with a luciferase reporter plasmid driven by the promoter region of *BiP* and a plasmid containing a reporter gene coding for β-galactosidase generously given by Prof. Mori (Yoshida et al., 2001). Cells were seeded in 12-well plates (Corning) at a density of 250,000 cells/well. Cells were co-transfected for 4 h with 0.5 μg of luciferase reporter plasmid, 0.75 μg of XBP1 plasmid, and 0.75 μg of DNA reporter plasmid using Superfect (Qiagen, Hilden, Germany). After 24 h post-transfection, cells were then incubated in the presence of 50 nM TG for 6 h or 500 nM BFA for 10 h. At the end of the incubation, medium was replaced by fresh DMEM medium containing 10% FBS for 18 or 14 h for TG- or BFA-treated cells, respectively. Luciferase activity was then measured by luminescence using a spectrofluorimeter. Positive and negative controls were cells co-transfected with a plasmid containing the luciferase reporter gene and an expression plasmid coding for an inactive (unspliced) or active form (spliced) of XBP1 (Yoshida et al., 2001). Results are expressed as relative luminescence units (RLU) normalized for β-galactosidase activity and represent the means ± SD for three independent experiments (n = 3).

Analysis of mitochondrial morphology

Cells were seeded in Lab-Tek II culture chambers (Nalge Nunc International, Lab-Tek Brand Products, NY) at a density of 20,000 cells per chamber. After 24 h, cells were incubated in the presence or in the absence of 50 nM TG or 500 nM BFA for different periods. At the end of the incubation time, media were removed and cells were washed with KRH buffer (Krebs–Ringer Hepes buffer:125 mM NaCl, 5 mM KCl, 1.3 mM $CaCl_2$, 1.2 mM $MgSO_4$, 25 mM Hepes, pH 7.4). Cells were then incubated for 30 min at 37°C with 100 nM Mitotracker® Green FM probe (Molecular Probes, Life Technologies) diluted in KRH + 2% BSA. Live cells

TABLE 1. List of antibodies used

Target	Manufacturer	Reference	Dilution
α-tubulin	Sigma–Aldrich	T5168	1:7500
β-actin	Sigma–Aldrich	A5441	1:7500
β-subunit ATP synthase	Molecular Probes, Life Technologies	A21350	1:1000
BiP/Grp78	BD Biosciences	610979	1:1000
Cytochrome c	BD Pharmingen	556433	1:1000
Drp1	BD Biosciences	611113	1:1000
eIF2α	Cell Signaling	9722	1:500
Fis1	Sigma-Aldrich	HPA017430	1:1000
HADHA	Abcam	ab54477	1:1000
IRE-1	Novus Biological	NB100-2324	1:1000
JNK	Cell Signaling	9252	1:1000
K63Ub	Cell Signaling	5621	1:1000
Mff	Sigma–Aldrich	HPA010968	1:5000
Mfn1	Sigma–Aldrich	WH0055669M4	1:1000
Mfn2	Abcam	ab50838	1:1000
Mfn2	Santa Cruz Biotechnology	sc-100560	1:1000
MiD49/SMCR7	ProteinTech	16413-1-AP	1:2000
MiD51/SMCR7L	ProteinTech	20164-1-AP	1:2000
MnSOD2	Merck Millipore	06-984	1:1000
mtHSP70	Enzo Life Sciences	ALX-804-077	1:1000
Opa1	BD Biosciences	612607	1:1000
Phospho-eIF2α	Cell Signaling	3597	1:200
Phospho-IRE-1	Novus Biological	NB100-2323	1:500
Phospho-JNK	Cell Signaling	9251	1:500
TOM20	BD Biosciences	612278	1:5000
TOM40	Santa Cruz Biotechnology	sc-11414	1:1000
PARP-1	BD Pharmigen	552597	1:1000
Caspase 3	Cell Signaling	9662	1:1000

were observed using confocal microscopy (TCS SP5 II, Leica Microsystems, Wetzlar, Germany). The length of the mitochondrial fragments was determined by calculating the aspect ratio (AR, defined as the major axis/the minor axis of mitochondrion) of mitochondrial objects in the entire cell sections using the Image J 64 software according to De Vos and Sheetz (2007). The degree of branching of the mitochondrial network was also calculated by measuring the form factor (defined as $[P_m^2]/[4\pi A_m]$), where P_m is the length of the mitochondrial outline and A_m is the area of the mitochondrion fragment (Mortiboys et al., 2008). Analyses were performed on at least 100 events/cell, $n \geq 40$ cells from three independent experiments.

Mitochondrial membrane potential and mitochondrial $O_2^{\bullet -}$ quantifications by flow cytometry

Mitochondrial membrane potential was assessed with TMRE (tetramethylrhodamine ethyl ester, perchlorate; Molecular Probes, Life Technologies) fluorescent probe in HepG2 cells incubated in the presence or in the absence of 50 nM TG or 500 nM BFA. Cells were seeded in 12-well culture plates (Corning, Inc.) at a density of 250,000 cells/well. At the end of the incubation with the ER stressors or after a recovery period of 18 or 10 h, cells were incubated for 30 min at 37°C with 25 nM TMRE. Cells were then rinsed with ice-cold PBS, trypsinized using trypsin-EDTA (Gibco, Life Technologies), centrifuged and resuspended in 500 μl of Hepes buffer (10 mM Hepes; pH 7.4, 150 mM NaCl, 5 mM KCl, 1 mM $MgCl_2.6H_20$). Cells were then rapidly analysed by flow cytometry with a FACScalibur (BD Biosciences), using the FL2-H channel. Data were processed using the BD CellQuest™ Pro software. MCFR (Mean Channel Fluorescence Ratio) was determined for each condition by calculating the ratio between the mean fluorescence intensity and the mean value of autofluorescence intensity measured for the corresponding unlabelled cells, used as negative controls. Results are expressed as relative fold change to the corresponding control and represent means ± SD for three independent experiments ($n = 3$).

The relative production of mitochondrial superoxide anion radicals was measured in HepG2 cells incubated as described above. At the end of the incubations, cells were loaded for 20 min at 37°C with 5 μM MitoSOX™ Red fluorescent specific dye (Molecular Probes, Life Technologies) diluted in complete HBSS (Hanks's Balanced Salt Solution) buffer (0.137 M NaCl, 5.4 mM KCl, 0.25 mM Na_2HPO_4, 0.44 mM KH_2PO_4; pH 7.4, 1.3 mM $CaCl_2$, 1.0 mM $MgSO_4$, 4.2 mM $NaHCO_3$). When indicated, antimycin A-treated cells (10 μM for 10 min) were used as positive controls and FCCP-treated cells (20 μM for 20 min) as negative controls. Cells were then rinsed with PBS, trypsinized using trypsin-EDTA (ethylenediaminetetraacetic acid) (Gibco, Life technologies), centrifuged, and resuspended in 500 μl of HBSS buffer. Cells were analysed by flow cytometry with a FACScalibur (BD Biosciences), using the FL2-H channel and data were processed using the BD CellQuest™ Pro software. MCFR was determined for each condition by calculating the ratio between the MitoSox mean fluorescence intensity and the mean value of autofluorescence intensity measured for the corresponding unlabeled cells, as a negative controls. Results are expressed as relative fold change to the corresponding control and represent means ± SD for three independent experiments ($n = 3$).

Mitochondria respiration assays

The extracellular flux Analyser XF96 (Seahorse Bioscience, North Billerica, MA) was used to measure the oxygen consumption rate (OCR) as described previously (Wanet et al., 2014) in HepG2 cells incubated with 50 nM TG or 500 nM BFA. The day prior to the assay, cells were seeded in an XF cell mito stress 96-well microplate at a density of 20,000 cells/well. A XF-cell mito stress test (Seahorse Bioscience) was performed according to the manufacturer's instructions and using the following chemical concentrations: 2 μM oligomycin, 0.5 μM FCCP (carbonyl cyanide 4-(trifluoromethoxy) phenylhydrazone), 1 μM antimycin A, and 1 μM rotenone. Once measurements were performed, cells were lysed in 0.5 N NaOH and OCR measurements were normalized to the protein content of the well. Basal respiration was calculated by substracting the non-mitochondrial oxygen consumption (OCR following the addition of both antimycin A and rotenone) to the basal OCR. For each condition, eight technical replicates were performed in two independent experiments.

ATP content determination

Cells were seeded in 6-well culture plates (Corning, Inc.) at a density of 500,000 cells/well. After 24 h, cells were incubated in the presence or in the absence of 50 nM TG or 500 nM BFA for different periods and followed by a recovery period. ATP content was measured using a luciferin–luciferase reaction assay. Cells were permealized for 10 s with 500 μl of ATP-releasing agent (Sigma–Aldrich). The solution was recovered and diluted 800 times in pure water before being incubated with an ATP assay mix solution (Sigma–Aldrich) at a 1:1 ratio (vol/vol). Relative light units, based on emitted photons were quantified using a luminometer (FB12 Luminometer from Berthold Detection Systems), and results were normalized for protein content determined by Folin assay.

Mitochondrial matrix calcium concentration measurement

Mitochondrial matrix calcium concentration ($[Ca^{2+}]_{mt}$) was measured in HepG2 cells with the Rhod-2 AM fluorescent probe (R1245MP, Molecular Probes, Life Technologies). Cells were seeded in a black 96-well Imaging plate (353219, BD Biosciences) at a density of 7,500 or 5,000 cells/well for short or long periods of time, respectively. After 24 h, cells were incubated in the presence or not of 50 nM TG or 500 nM BFA diluted in fresh complete medium for different incubation and recovery periods. For the last 60 min, 5 μM Rhod-2 AM probe was added to the medium. Cells were rinsed with complete medium (DMEM + 10% FBS) and fluorescence was measured with a BD pathway 855 bioimager (BD Biosciences). To measure the mitochondrial calcium concentration, micrographs of labeled cells were taken and the image was segmented in such a way that each cell represents a ROI (region of interest). Fluorescence was then measured in each ROI and the mean calculated for each well for each condition. The results were expressed as fluorescence (AU, Arbitrary Units) representing means ± SD. For each condition, eight technical replicates were performed in three independent experiments.

Gene expression and real-time RT-qPCR (reverse transcription-quantitative PCR)

HepG2 cells were seeded at a density of 1.10^6 cells in 25 cm^2 culture dishes (Corning, Inc.). The next day, cells were incubated in the presence or not of 50 nM TG or 500 nM BFA for different periods of time as described before. Total RNA was extracted using QIAGEN RNeasy mini kits and QIAcube equipment (Qiagen, Venlo, the Netherlands) according to the manufacturer's instructions. An equivalent of 1 μg total RNA was then reverse transcribed into mRNA using the cDNA first strand synthesis kit Transcriptor First Hand cDNA synthesis kit (Roche Applied Science, Pensberg, Germany). RT-qPCR was performed using SYBR Green PCR Master mix (Roche), and the Fis1-F, 5′-AATGATGACATCCGTAAAGGC-3′ (Integrated DNA Technologies, Coralville, IA) and 23 kD-F, 5′-GCCTACAAGAAAGTTTGCCTATCTG-3′ (Integrated DNA Technologies) primers (designed using Primer Express 1.5 software) used at the optimal concentration in an ABI 7900 HT

Fast Real Time PCR System (Applied Biosystem, Thermo Fisher Scientific Leusden, The Netherlands). The process starts by a 10 min 95°C hold stage, followed by the PCR stage (40 cycles at 95°C for 15 sec and 60°C for 1 min) and ends by the melting curve stage (95°C for 15 sec, 60°C for 1 min, and 95°C for 15 sec) by using an ABI PRISM 7000 SDS thermal cycler (Applied Biosystems).

All results were normalized to the mRNA abundance of the 23 kD used as the reference gene. Relative mRNA abundance was quantified using the threshold cycle method (2-ΔΔCt method) and expressed relatively to control cells (de Longueville et al., 2003).

Statistical analyses

Data from at least three independent experiments is presented as means ± SD and the significance of differences between means was evaluated by two-way ANOVA, using the Holm–Sidak tests as determined by the software SigmaStat (Jandle Scientific, Erkrath, Germany). Differences between means were only considered statistically significant when $P < 0.05$ or less.

Results

Set up of conditions in which TG and BFA activate UPR without inducing apoptosis

In order to study the impact of a sublethal ER stress on the mitochondrial population, we first set up a model in which UPR activation could be activated without major signs of cell death. HepG2 cells were thus incubated with different concentrations of thapsigargin (TG) or brefeldin A (BFA), two widely used ER stressors (Lee et al., 2012; Moon et al., 2012; Foldi et al., 2013; Win et al., 2014) and we assessed the cytotoxicity by a LDH release assay (Fig. 1A). TG induces LDH release in a concentration-dependent way ranging between 7% (25 nM) and 15% (100 nM), whereas the positive control, corresponding to HepG2 cells treated with 50 μM etoposide, reached 20.5%. When cells are incubated with BFA (50–500 nM), no toxicity was observed as the percentages of LDH release remained under 5% whatever the concentration tested (Fig. 1A). We next looked for the activation of ER stress markers in HepG2 cells incubated with TG (Fig. 1B) or BFA (Fig. 1C). The phosphorylation of the translation initiation factor eIF2α (phospho-eIF2α) is slighlty increased in cells incubated for 6 h with TG at least at the highest concentrations, but the phosphorylation was transient and not maintained after a 18 h recovery period (Fig. 1B). The phosphorylation of eIF2α is also more pronounced in cells incubated with BFA for 10 h than in TG-treated cells, but again, barely dectable at the end of a 14 h recovery period (Fig. 1C). The abundance of BiP was also increased in cells incubated with TG (Fig. 1B) or BFA (Fig. 1C) but only after the recovery periods. However, even if we observe an increase in the abundance of BiP/Grp78 protein in cells exposed to a recovery period, we were unable to determine whether it is due to the recovery period itself or if it would have been observed for a prolonged incubation time with the molecule as this could not be tested without increasing dramatically the toxicity. The overexpression of the chaperone seems thus delayed in TG- and BFA-exposed cells (Fig. 1B and C). To confirm the activation of the UPR in cells exposed to TG or BFA, HepG2 cells were transiently co-transfected with a luciferase reporter plasmid driven by the promoter of *BiP* (Yoshida et al., 2001) (Fig. 1D). We observed an increased activation of the BiP promoter in cells incubated with BFA from 50–500 nM (Fig. 1D). The activation measured in TG-treated cells was more pronounced and even stronger than in the positive control cells co-transfected with a plasmid containing the luciferase reporter gene and an expression plasmid coding for an active form (spliced) of XBP1 (Fig. 1D).

Based on these results, we selected 50 nM TG for 6 h and 500 nM BFA for 10 h, followed or not by a recovery period without stressor, to induce sublethal ER stress. We further checked the absence of apoptotic markers in cells incubated in these conditions by assessing the status of cleaved PARP-1 and cleaved caspase-3 (Supporting Information Fig. S1A) as well as DNA fragmentation (Supporting Information Fig. S1B). Even if we observed a very slight cleavage of caspase-3 in cells incubated 6 h with TG followed by 18 h of recovery, for the other conditions, we did not observe any cleavage of neither caspase-3 nor PARP-1 and were unable to detect any increase in DNA fragmentation in HepG2 cells incubated with either TG or BFA, whether the markers were analyzed readily after the incubation with the stressor or after a recovery period up to 2 days after the beginning of the incubation with the ER stressor. Cells incubated with 50 μM etoposide for 16 h and maintained 2 days before the analysis of the markers showed caspase-3 and PARP-1 cleavage as well as a strong DNA fragmentation (Supporting Information Fig. S1A and B).

As it has been reported that some UPR markers might be very rapidly activated (Prostko et al., 1993; DuRose et al., 2006), we also studied the abundance of BiP and the phosphorylated forms of either eIF2α (P-eIF2α) or IRE1 (P-IRE1) in cells incubated for shorter periods with the ER stressors. We observed a statistical increase in P-eIF2α in cells incubated with BFA as soon as 1 h after the addition of the molecule and the phosphorylation was sustained for up to 10 h but disappeared after the recovery period (Fig. 2A). In these conditions, the abundance of the phosphorylated form of IRE1 was significantly increased after a long period (10 h) of incubation with BFA, whereas the abundance of BiP in BFA-treated cells was only increased after the recovery period (Fig. 2A). The effect of TG on the activation of UPR markers was faster and stronger as a phosphorylation of eIF2α and IRE1 was already found after 30 min of incubation (Fig. 2B). The abundance of P-eIF2α decreased progressively over time whereas P-IRE1 gradually increased for up to 6 h of incubation and was completely lost after the recovery period. The abundance of BiP was only increased during the recovery period in TG-treated cells (Fig. 2B). In conclusion, these results indicate that it is possible to activate a mild and transient UPR stress response with TG or BFA that triggers rapidly the phosphorylation of eIF2α and IRE1 and is compatible with cell survival. However, in these conditions, as shown in Figures 1 and 2, it takes longer to detect an increase in the abundance of BiP, a step reported to be necessary for the cells to cope with the stress (Fu et al., 2007; Lin et al., 2007; Walter et al., 2015).

Sublethal ER stress induces mitochondrial fragmentation

It is generally accepted that induction of a severe and prolonged ER stress triggers apoptosis and has a dramatic impact on the mitochondrial population (Deniaud et al., 2008; Zhang et al., 2008; Cosentino and Garcia-Saez, 2014). However, the effect of a transient and sublethal ER stress on mitochondria is still largely unknown. As mitochondrial modifications observed before apoptosis are usually dealing with mitochondrial dynamics disturbances and, more specifically, fragmentation (Hom et al., 2007; Cosentino and Garcia-Saez, 2014; Iqbal and Hood, 2014), we first decided to analyze the putative effect of a non-lethal ER stress on mitochondrial morphology. Mitochondrial network morphology was assessed by fluorescence confocal microscopy in cells incubated or not with the ER inducers, stained with 100 nM MitoTracker Green, a fluorescent probe that specifically stains mitochondria regardless of the membrane potential (Pendergrass et al., 2004) (Fig. 3A). Control cells display an elongated and interconnected mitochondrial network whereas cells incubated with TG or BFA display a more fragmented mitochondria population with accumulation of rod-like structures. Quantitative analysis of these observations demonstrated a highly significant decrease

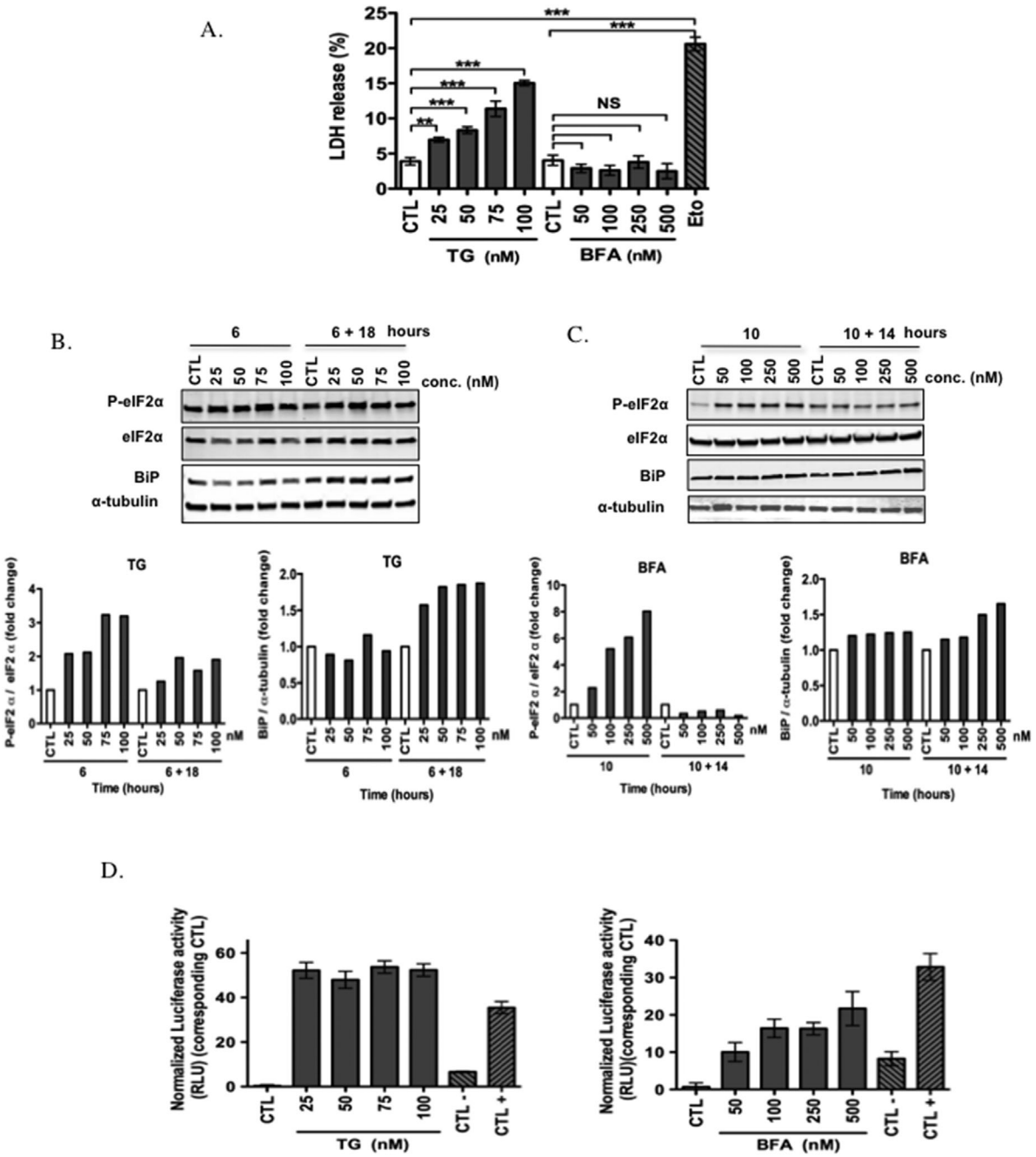

Fig. 1. Induction of the Unfolded Protein Response (UPR) using thapsigargin and brefeldin A. HepG2 cells were incubated with 25–100 nM thapsigargin (TG) or with 50–500 nM brefeldin A (BFA) for 6 or 10 h, respectively. LDH release assay was assessed after 42 or 38 h of recovery following the incubations with TG or BFA, respectively. Etoposide 50 μM for 16 h followed by a recovery period of 32 h was used as a positive control. Results represent means ± SD for three independent experiments and are expressed in percentages of release. NS: not significant; **, *: significantly different from CTL cells with $P < 0.01$ or < 0.001, respectively. B: Cells were incubated with 25–100 nM TG for 6 h followed or not by a recovery period and the abundance of UPR markers (phospho-eIF2α and BiP) was analyzed by Western blot. Signal intensity was quantified and normalized to the abundance of α-tubulin (loading control) and results are expressed in fold change, n = 1. C: Cells were incubated with 50–500 nM BFA for 10 h followed or not by a recovery period and the abundance of UPR markers (Phospho-eIF2α and BiP) was analyzed by Western blot. Signal intensity was quantified and normalized to the abundance of α-tubulin (loading control) and results are expressed in fold change, n = 1. D: In some conditions, HepG2 cells were co-transfected with a luciferase reporter plasmid driven by the promoter region of *BiP* and a plasmid containing a reporter gene coding for β-Galactosidase. Cells were incubated with 25–100 nM TG or 50–500 nM BFA for 6 or 10 h and followed by a recovery period of 14 or 18 h, respectively. Luciferase activity was measured by fluorescence. CTL− and CTL+ conditions represented negative and positive controls for which cells were co-transfected with a plasmid containing the luciferase reporter gene and an expression plasmid coding for an inactive (unspliced) or an active form (spliced) of XBP1. These cells used as negative and positive controls were thus transfected but not exposed to TG or BFA. Results are expressed as relative luminescence units (RLU) normalized for β-Galactosidase activity and represent the means ± SD for three independent experiments (n = 3).**

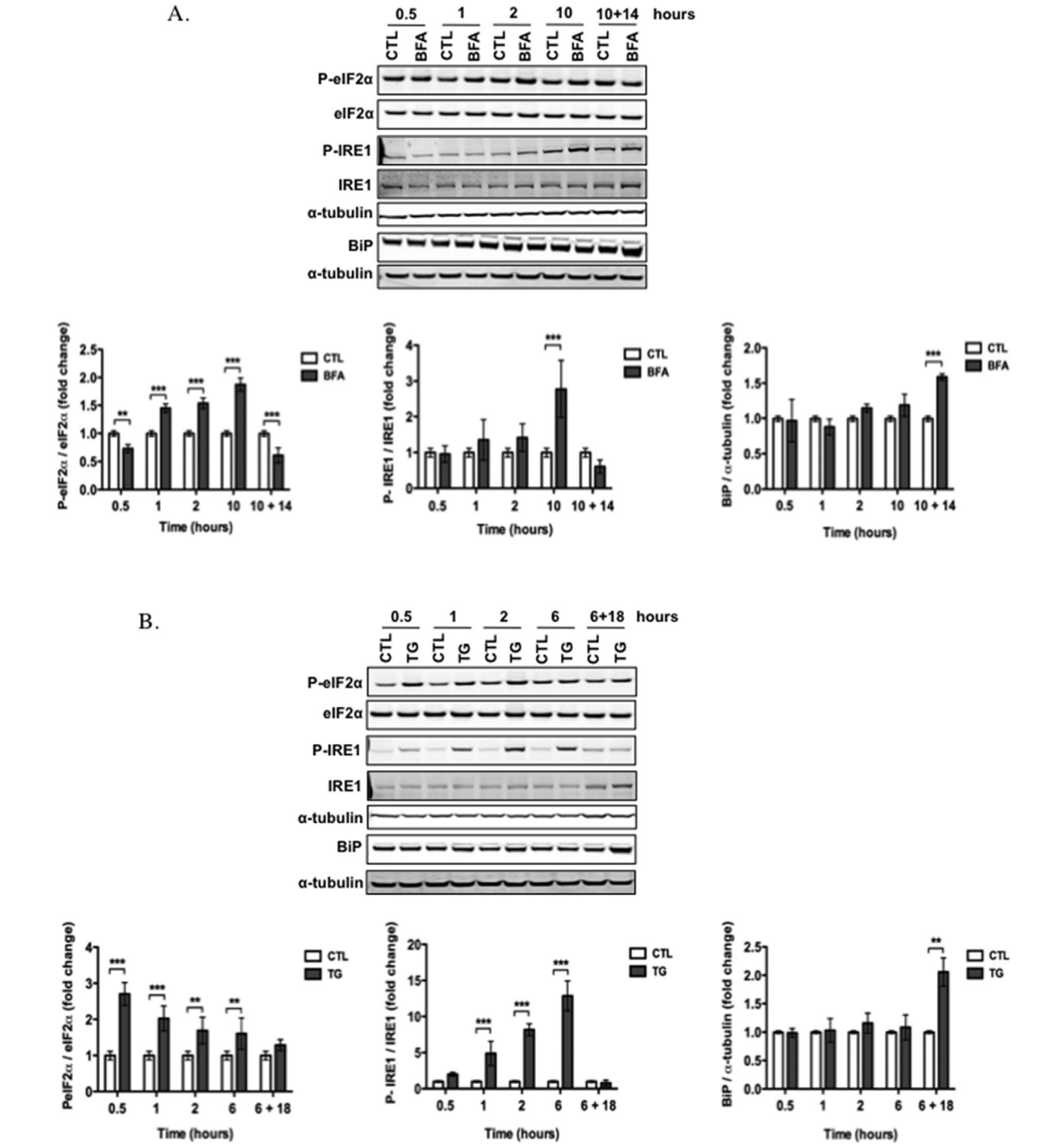

Fig. 2. Early UPR activation after TG- or BFA-induced ER stress. A: Cells were incubated with 500 nM BFA for 0.5, 1, 2, or 10 h or for 10 h followed by a 14 h recovery period. B: Cells were incubated with 50 nM TG for 0.5, 1, 2, or 6 h or for 6 h followed by a 18 h recovery period. A and B: The abundance of several UPR markers (Phospho-eIF2α, phospho-IRE1 and BiP) was analyzed by Western blot. Signal intensity was quantified and normalized to the abundance of α-tubulin (loading control). Results are expressed in fold change and represent means ± SD (n = 3).

in the the elongation of mitochondria (aspect ratio, $P < 0.01$ or 0.001) and in mitochondrial branching (form factor, $P < 0.001$), in TG- or BFA-treated cells (Fig. 3B). We also have to notice that the slight but highly significant increase in fragmentation of the mitochondria is a very rapid phenomenon that occurs within the first 30 min of incubation with the stressors, and is transiently prolonged during the recovery periods as illustrated in Figure 3. However, when cells treated with TG for 6 h or BFA for 10 h are allowed to recover for longer periods of time (66 and 62 h, respectively), the morphology of mitochondria is back to normal (data not shown). Although we do not have the explanation for the prolonged changes of mitochondria

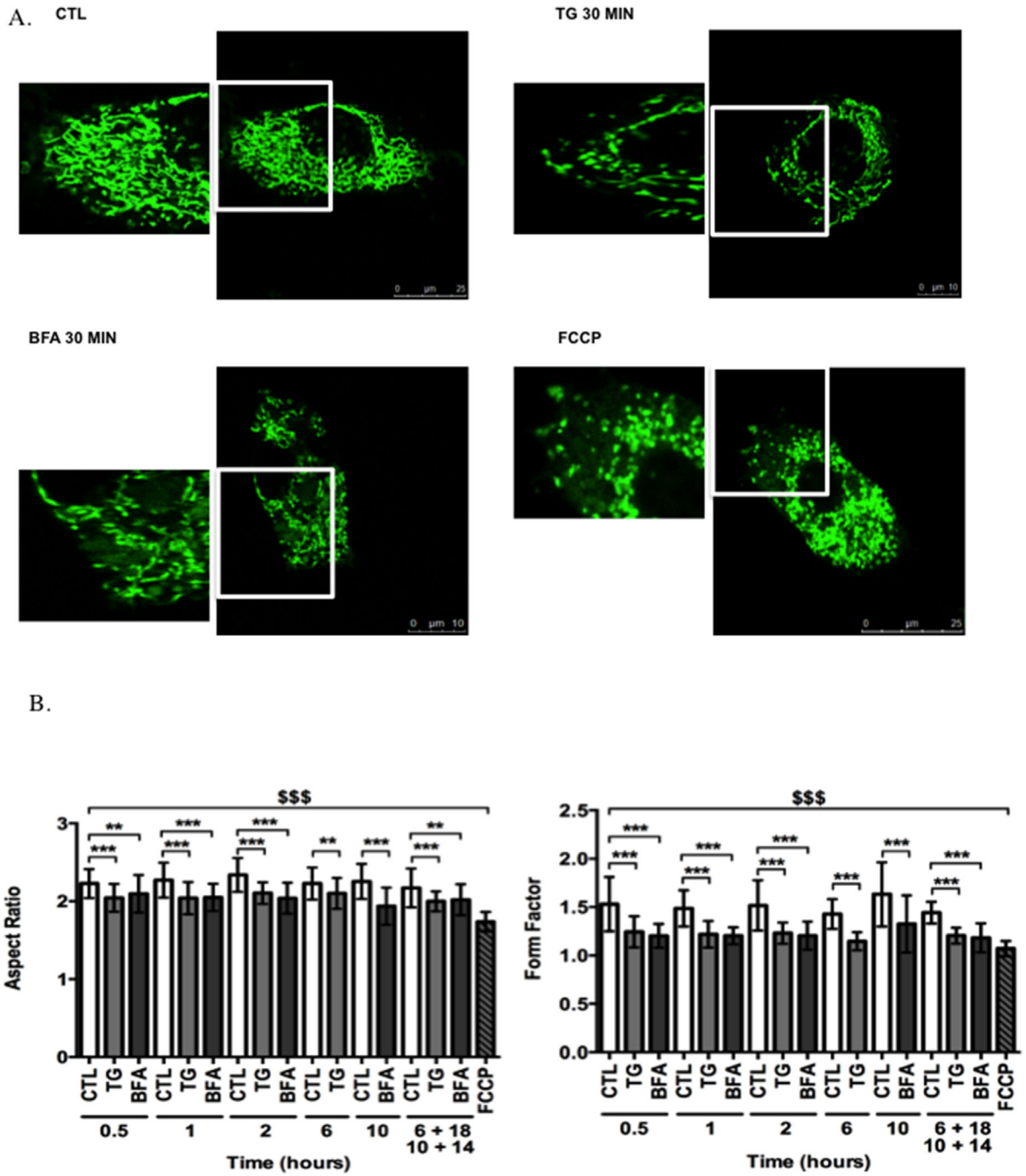

Fig. 3. Sublethal ER stress induces mitochondrial fragmentation. A: Representative confocal micrographs of mitochondrial morphology displayed after staining with 100 nM Mitotracker Green in HepG2 cells incubated in the presence or not of 50 nM TG or 500 nM BFA for different periods of time (0.5, 1, 2, and 6 or 10 h, followed or not by a recovery period of 18 or 14 h, respectively). FCCP at 20 μM was used for 30 min as a positive control for inducing mitochondrial fragmentation. B: The length or the degree of branching of the mitochondrial fragments was characterized by determining the Aspect Ratio (AR) or the Fom factor (FF) on micrographs using the ImageJ 64 software as described in the Materials and Methods section. Results are expressed as aspect ratio and represent means ± SD (at least 100 events/cell, n ≥ 40 cells from three independent experiments). **, *, or $$$: significantly different from CTL cells with $P < 0.01$ or < 0.001, respectively.**

morphology in response to transient sub-lethal ER stress inducers, kinetic and dynamic aspects of molecular effectors controlling fusion and fission events might be taken into account in the delayed response observed on mitochondria morphology. As a positive control, cells were pre-incubated for 30 min with 20 μM FCCP, an uncoupling agent known to induce a strong fragmentation of the mitochondrial network in HeLa and CV1 cells (Pletjushkina et al., 2006) and thus a lower aspect ratio and form factor (Fig. 3B). These observations allowed us to conclude that even a short, non-lethal ER stress has an important effect on mitochondrial morphology, reflected by an increase in mitochondria fragmentation.

Sublethal ER stress affects mitochondrial functions

Whether mitochondrial fragmentation is a cause or a consequence of apoptosis is still under debate (Breckenridge et al., 2003; Karbowski et al., 2004; Hom et al., 2007). However, it is well demonstrated that fragmentation of the mitochondrial population is accompanied with changes in mitochondrial membrane potential and in mitochondrial Ca^{2+} loading, suggesting mitochondrial dysfunctions.

We first analyzed, by Western blot, the abundance of several mitochondrial proteins that exert various mitochondrial functions such as mt-HSP70 (translocation and folding of imported proteins), the β-subunit of ATP synthase (oxidative phosphorylation), HADHA (hydroxyacyl-CoA dehydrogenase/3-ketoacyl-CoA thiolase/enoyl-CoA hydratase) (fatty acid β-oxidation), or SOD2 (superoxide dismutase 2) (antioxidant activity) in HepG2 cells incubated with 50 nM TG or 500 nM BFA for 6 or 10 h, followed by a recovery period of 42 or 38 h, respectively, but no effect on the abundance of these proteins could be detected, no matter what the condition of interest (Supporting Information Fig. S2).

As it was demonstrated that, during the adaptive response to ER stress, modifications of mitochondrial bioenergetics could be detected before apoptosis (Bravo et al., 2011), we next decided to analyze the putative impact of a sublethal ER stress on mitochondrial membrane potential, respiration and ATP content (Fig. 4A–C).

First, the mitochondrial membrane potential was analyzed by flow cytometry on cells treated with 50 nM TG or 500 nM BFA and loaded with 25 nM TMRE. As shown in Figure 4 A, the mitochondrial membrane potential is rapidly (from 30 min of incubation) and significantly decreased in cells incubated in the presence of TG while the reduction of mitochondrial membrane potential is only observed later in BFA-treated cells. After the recovery period, it is important to emphasize the fact that a lower mitochondrial membrane potential is still observed for BFA-treated cells (14 h of recovery) while the membrane potential is back to normal in cells incubated with TG after 18 h of recovery. As a positive control, cells have been incubated with FCCP, a protonophore, that uncouples mitochondrial respiration from ATP production (Luvisetto et al., 1987) triggering a strong decrease in the mitochondrial membrane potential (Fig. 4A).

To investigate the impact of a non-lethal and transient TG- or BFA-induced ER stress on mitochondrial respiration, we examined the real-time oxymetric changes (mitochondrial oxygen consumption rate in time [OCR]) using a Seahorse XF96 bioenergetic analyzer. OCR was measured in basal condition, after the addition of oligomycin A (an ATP synthase inhibitor) in order to evaluate the coupling efficiency of the respiratory chain, in the presence of FCCP (to evaluate the spare repiratory capacity of cells), and with a combination of antimycin A and rotenone (inhibitors of mitochondrial complexes III and I, respectively). All these conditions were performed in order to calculate and substract the non-mitochondrial oxygen consumption from measurements (Supporting Information Fig. S3A and B) (Brand and Nicholls, 2011). We found that the basal respiration was rapidly but transiently decreased in TG-treated cells (50 nM) when compared with control cells (Fig. 4B). Indeed, after a 6 h treatment, OCR was back to normal and even increased after a recovery period of 18 h. Similarly, basal respiration was decreased in cells incubated for 1 h with 500 nM BFA, while the oxygen consumption in cells treated for 10 h is increased and still slightly increased after a 14 h recovery period (Fig. 4B). Moreover, the coupling efficiency, representing the fraction of the basal respiration that is used for ATP production presented the same pattern (data not shown). Together, these results demonstrate that, rapidly after the initiation of a non-lethal and sublethal ER stress, cells seem to reduce oxygen consumption while, when adapted to the ER stress or during recovery, cells have a more efficient OXPHOS system. In addition to the OCR assessment, we also analyzed the ECAR (extracellular acidification rate), but no differences between control versus TG- or BFA-treated cells could be observed over the time (Fig. 4B). We also measured cellular ATP content in cells treated with TG or BFA, but no changes could be observed in the ATP content in BFA-treated cells while a significant increase in the ATP content was observed only in cells incubated in the presence of TG for 6 h followed by a recovery period of 18 h (Fig. 4C). Cells exposed to a non-lethal and transient ER stress do not see their ATP content decreased, an observation that could be explained by either the maintenance of ATP production, a compensating glycolytic activation (unlikely as the acidification of the extracellular media is not observed) or the adjustment and reduction of the ATP-dependent processes preventing ATP consumption and thus sparing ATP content.

Effects of a sublethal ER stress on mitochondrial calcium concentration $[Ca^{2+}]_{mt}$ and mitochondrial superoxide anion radicals (mt $O_2^{\bullet -}$) production

Because a reduced mitochondrial membrane potential might affect the mitochondrial Ca^{2+} buffering capacity and/or mitochondrial $mtO_2^{\bullet -}$ production (Eom et al., 2010; Joshi and Bakowska, 2011), we first quantified the mitochondrial matrix calcium concentration $[Ca^{2+}]_{mt}$, using the fluorescent Rhod-2 probe (Fig. 5A). A significant increase in the $[Ca^{2+}]_{mt}$ in cells exposed to 50 nM TG was observed even after the recovery period while no change could be detected in $[Ca^{2+}]_{mt}$ in BFA-treated cells (Fig. 5A). We also measured the cytosolic calcium concentration in HepG2 cells treated for 1, 5, and 10 min with 50 nM TG or 500 nM BFA and pre-loaded with Rhod-3, a fluorescent probe used to capture rapid changes in cytosolic calcium concentration and quantified the fluorescence intensity in a BD pathway TM 855. As expected, we observed that the free cytosolic calcium concentration ($[Ca^{2+}]_c$) is rapidly increased in TG-treated cells while no increase and even a slight decrease in $[Ca^{2+}]_c$ is found in BFA-treated cells (data not shown).

We next quantified the mitochondrial production of $mtO_2^{\bullet -}$ in TG- or BFA-treated cells using the MitoSOX™ fluorescent dye (Fig. 5B). We found that the production/abundance of $mtO_2^{\bullet -}$ is lower in TG-treated cells (Fig. 5B). The rapid and significant reduction of $mtO_2^{\bullet -}$ detection is correlated with the reduction in mitochondrial membrane potential observed for HepG2 cells exposed to TG (Fig. 4A). In BFA-treated cells, a significant decrease in $mtO_2^{\bullet -}$ production was also observed but the decrease was less severe and only observed after a longer incubation period (1 h vs. 30 min for TG) (Fig. 5B). As positive and negative controls, cells were incubated for 15 min with 10 μM antimycin A, an inhibitor of the complex III of the respiratory chain known to induce $mtO_2^{\bullet -}$ production (Chen et al., 2003) or for 30 min with 20 μM FCCP, a mitochondrial uncoupler known to reduce $mtO_2^{\bullet -}$ production in vitro and in vivo (Caldeira da Silva et al., 2008; Guimaraes et al., 2012) (Fig. 5B).

Sublethal ER stress induces mitochondrial fragmentation but does not depend on changes in the abundance of proteins involved in fusion/fission mechanisms

In order to get a better insight in the mechanisms involved in mitochondrial fragmentation caused by a mild ER stress, we studied the abundance of the different keyplayers described to regulate the dynamics of the mitochondrial network (Mishra

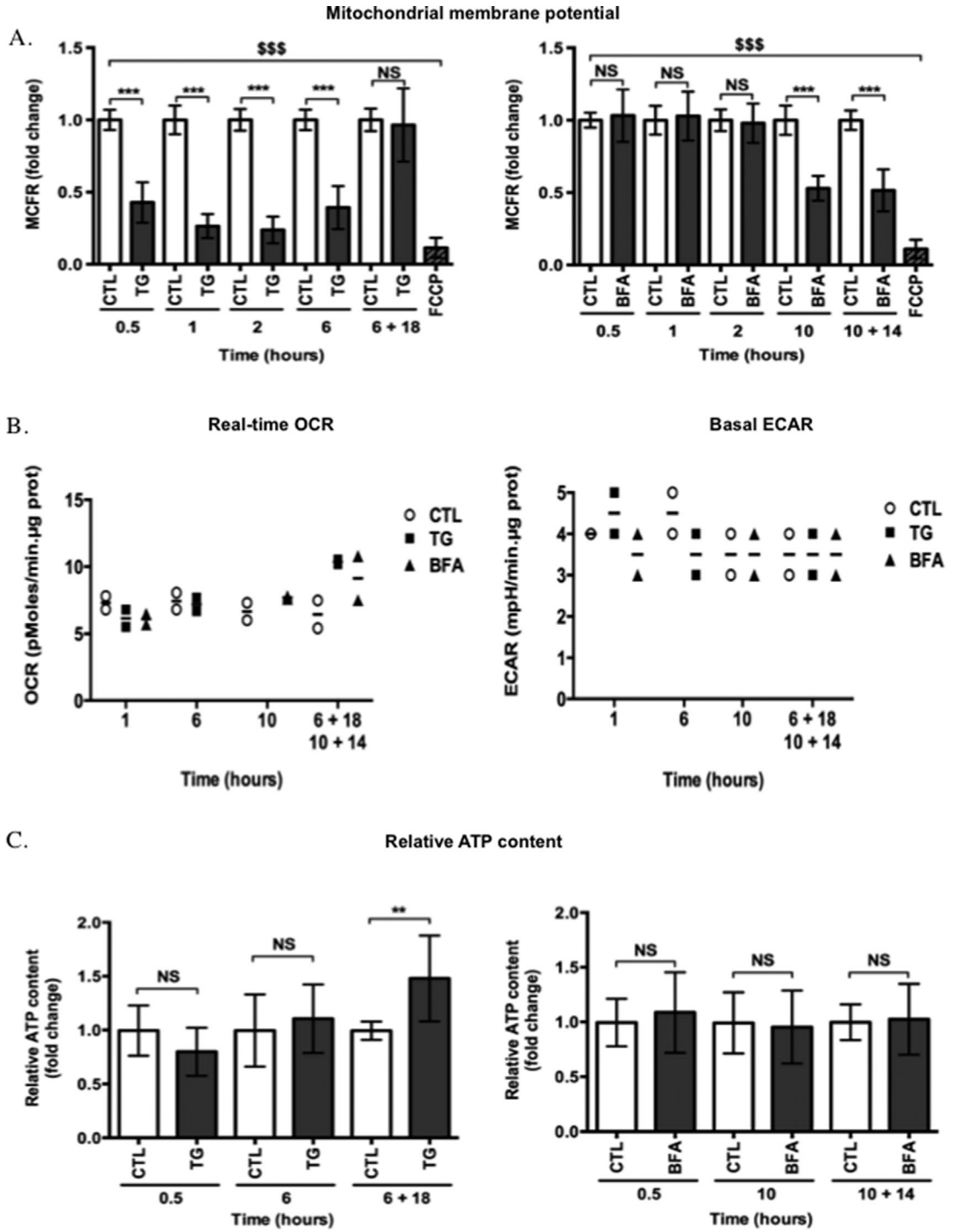

Fig. 4. Sublethal ER stress affects mitochondrial functions. A: The mitochondrial membrane potential was analysed in HepG2 cells incubated with 50 nM TG or 500 nM BFA for different periods of incubation, followed or not by a recovery period, using the specific mitochondrial membrane potential probe TMRE. Cells were stained or not (to allow autofluorescence determination from cells without dye) with 25 nM TMRE for 30 min and fluorescence was analysed by flow cytometry. Results are expressed as MCFR and are presented as means ± SD (n = 3). NS: not significant; *: significantly different from CTL cells with $P < 0.001$. B: OCR changes in response to oligomycin, FCCP, and antimycin A in combination with rotenone were used to calculate the basal respiration in HepG2 cells treated with 50 nM TG or 500 nM BFA for different periods of incubation, followed or not by a recovery period. Data is presented as average OCR in pMoles/min.µg (n = 2 independent experiments, eight wells for each condition). C: The ATP content was determined in HepG2 cells incubated with 50 nM TG or 500 nM BFA for different periods of incubation, followed or not by a recovery period. The ATP content was estimated using the luciferin–luciferase reaction assay as described in the Materials and Methods section. The ATP content, expressed relatively to the control cells, is presented as means ± SD (n = 3). NS: not significant; **: significantly different from CTL cells with $P < 0.01$.**

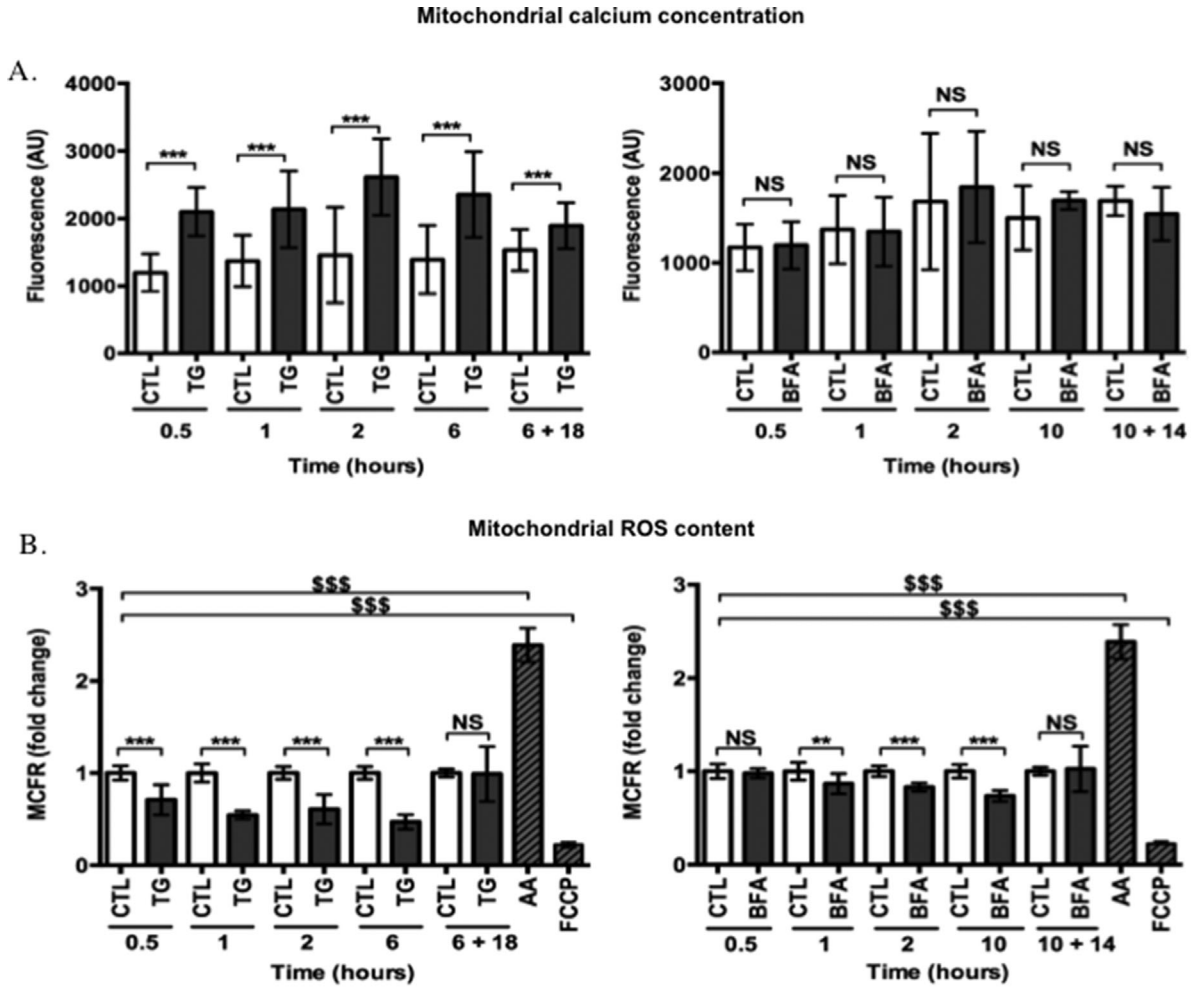

Fig. 5. Sublethal ER stress affects mitochondrial calcium concentration $[Ca^{2+}]_{mt}$ and mitochondrial $O_2^{\bullet-}$ ($mtO_2^{\bullet-}$) production. A: The mitochondrial calcium concentration was measured in HepG2 cells incubated with 50 nM TG or 500 nM BFA for different periods of incubation, followed or not by a recovery period, using the specific Rhod-2 AM probe. In the last 60 min of incubation, cells were stained with 5 μM Rhod-2 AM and fluorescence was measured with a BD pathway 855 bioimager. Results are expressed as Fluorescence (AU) and represent means ± SD (n = 3). NS: not significant; *: significantly different from CTL cells with $P < 0.001$. B: The $mtO_2^{\bullet-}$ production was assessed in HepG2 cells incubated with 50 nM TG or 500 nM BFA for different periods of incubation, followed or not by a recovery period, using the specific mitochondrial MitoSOX™ Red dye. Cells were stained or not (to allow autofluorescence determination from cells without dye) with 5 μM MitoSOX™ Red dye for 20 min. Fluorescence was measured by flow cytometry. As a positive control, cells were incubated with 10 μM antimycin A for 10 min while cells incubated with 20 μM FCCP for 20 min were used as a negative control. Results are expressed as fluorescence MCFR and are presented as means ± SD (n = 3). NS: not significant; **, ***: significantly different from CTL cells with $P < 0.01$ or with $P < 0.001$, respectively.**

and Chan, 2014; Roy et al., 2015). The abundance of Fis1 (Fig. 6A–C) and Drp1 (controlling fission events), and Mfn1, Mfn2, and Opa1 (regulating fusion events) was quantified by Western blotting and RT-qPCR. The analyses revealed no changes in the total abundance of mitochondrial fission proteins (Fis1, Drp1) or fusion proteins (Mfn1, Mfn2 and Opa1) in HepG2 cells incubated with TG (Fig. 6A and Supporting Information Fig. S4A). In addition, no changes at the mRNA level of these fission and fusion effectors were observed (data not shown). In BFA-treated cells, we only observed a significant difference in the abundance of Fis1 protein for cells incubated for 10 h followed by a 14 h recovery period (Fig. 6B and Supporting Information Fig. S4B) while a significant difference at the mRNA level is already observed after a 10 h incubation with the molecule (Fig. 6C). Based on these results, we hypothesized that mitochondrial fragmentation observed in BFA-treated cells might result from a fission mechanism rather than from a lack of fusion events. Because the mechanism of mitochondrial fission could be due to the recruitment of cytosolic Drp1 at the outer mitochondrial membrane by Fis1 (Yu et al., 2005), we wondered whether Drp1 could be differentially targeted to mitochondria in cells incubated with the ER-stress inducers even in the absence of a change in total Drp1 abundance. To test this hypothesis, we looked for a putative co-localization between Drp1 and Fis1. Semi-quantitative analysis of co-localization (using the ImageJ 64 software) in cells incubated with BFA and immunostained for these proteins revealed no change in the recruitment of Drp1 by Fis1 (Supporting Information Fig. S5A and B). These results suggest that increased mitochondrial fragmentation in ER-induced stress cells is unlikely to be the consequence of an increased recruitment of Drp1 at the OMM. While several post-translational modificiations, such as phosphorylation of Ser 616 (Qi et al., 2011; Strack et al., 2013; Cho et al., 2014; Yu et al.,

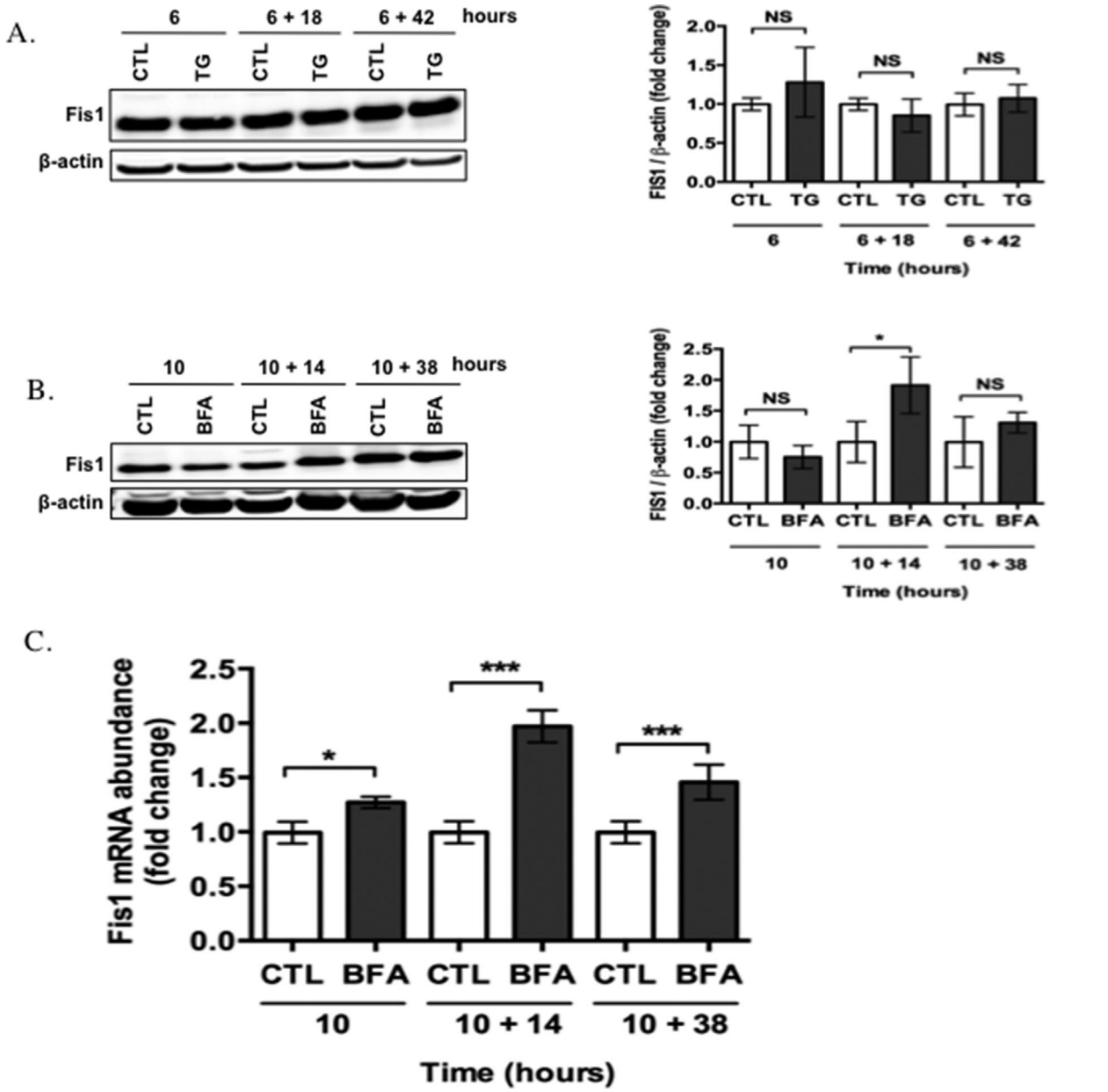

Fig. 6. Effects of a sublethal ER stress on the abundance of major regulators of mitochondrial dynamics. A: The abundance of Fis1 was determined by fluorescence Western blot analysis on 15 μg of clear cell lysates prepared from HepG2 cells incubated in the presence or in the absence of 50 nM TG (A) or of 500 nM BFA (B) for 6 or 10 h, respectively, followed or not by a recovery period. Fluorescent signal intensity was quantified and normalized to the abundance of β-actin (loading control). Results are expressed in fold change and represent means ± SD (n = 3) (A) (n = 4) (B). NS: not significant; *: significantly different from CTL cells with $P < 0.05$. C: Total RNA was extracted from HepG2 cells incubated with 500 nM BFA for 10 h and followed by a recovery period, reverse transcribed, and amplified by real-time RT-qPCR in the presence of Fis1 primers and SYBR green. 23 kDa was used in the calculation as a reference gene for data normalization. Results are expressed in fold change and represent means ± SD (n = 3), * or *: significantly different from CTL cells with $P < 0.05$ or <0.001, respectively.**

2011) or Ser 637 (Chang and Blackstone, 2007; Cereghetti et al., 2008) have been identified to control the function of Drp-1 in mitochondria fragmentation, we could not observe any changes in the phosphorylation status of Drp1 on these two residues in HepG2 cells incubated with TG or BFA (data not shown).

In order to determine whether Fis1 plays a role in the fragmentation of the mitochondrial network in cells incubated with the ER-stress inducers, we silenced the expression of Fis1 using a siRNA approach. Western blotting analysis revealed a strong decrease in the abundance of Fis1 protein in HepG2 cells 24 h post-transfection with a pool of four specifics siRNAs (siFis1) when compared with a control pool of siRNA (siRF) (Supporting Information Fig. S6A). However, the inhibition of Fis1 expression did not reverse the mitochondrial fragmentation observed in TG- or BFA-treated cells (Supporting Information Fig. S6B and C).

As Fis1 does not seem to play a role in the fragmentation observed in HepG2 cells exposed to ER-stress inducers, we next decided to study the abundance of the other fission actors

that could interact with Drp1, such as Mff, Mid49, and Mid51 as it has been recently reported that in eukaryotic cells, Fis1 might not be the major effector of fission (Otera et al., 2010; Palmer et al., 2013). Because these proteins are known to be anchored in the OMM, we performed Western blotting analyses on mitochondria-enriched fractions, expecting a change in the abundance of these proteins (Supporting Information Fig. S7). However, no changes in the mitochondrial abundance of these proteins could be found in BFA-treated cells when compared with control cells. As no changes in the abundance of these proteins was observed, we did not look further for their possible co-localization with Drp1.

Involvement of JNK phosphorylation in ER stress-induced changes of mitochondrial $O_2^{\bullet -}$ content and morphology

Several signaling pathways have been reported to link ER stress and mitochondrial dependent cell death pathways (Vannuvel et al., 2013). Among them, the IRE-1-TRAF2-ASK1-JNK pathway has recently been shown to impair mitochondrial respiration and decrease $mtO_2^{\bullet -}$ production triggering apoptosis by a mechanism dependent on the interaction with Sab (SH3 homology associated BTK binding protein) (Win et al., 2014).

As shown in Figure 2, we observed a rapid and strong phosphorylation of IRE1 in cells treated with TG (Fig. 2A) and a moderate phosphorylation of IRE1 in BFA-treated cells (Fig. 2B). Therfore, we analyzed, by Western blot, the abundance of the phosphorylated 46 and 54 kDa forms of JNK in lysates of cells incubated or not with 50 nM TG or 500 nM BFA for different incubation times followed or not by a recovery period of 18 or 14 h, respectively (Fig. 7A and B). A strong and rapid phosphorylation of JNK was observed for cells incubated with TG (Fig. 7A) that perfectly correlates with the rapid and strong activation of the IRE1 pathway (Fig. 2A). A less strong and more transient phosphorylation of JNK is also observed in cells incubated with BFA (Fig. 7B).

To assess the involvement of JNK phosphorylation on ER stress-induced mitochondrial morphological and functional modifications, we pre-treated the cells for 1 h with 40 μM SP600125, a well described JNK inhibitor (Bogoyevitch and Arthur, 2008). In these experimental conditions, a complete inhibition of JNK phosphorylation was observed (data not shown). We then evalutated the effects of the JNK inhibitor on the changes in mitochondrial membrane potential, mitochondrial $O_2^{\bullet -}$ production, and morphology in cells treated with the ER stressors (Fig. 8A–C, respectively). No effect of JNK inhibition on the decrease of mitochondrial membrane potential could be observed in cells treated with TG while a slight (but significant) reduction was found for cells treated with BFA (Fig. 8A). Importantly, the inhibition of JNK seems to limit the decrease in mitochondrial $O_2^{\bullet -}$ production in cells incubated with TG or BFA. In cells treated with BFA, even if the decrease in $mtO_2^{\bullet -}$ content is less severe, the recovery is almost complete when JNK phosphorylation is inhibited while the JNK inhibitor only slightly (by 10–20%), but significantly, reduces the decrease in $mtO_2^{\bullet -}$ production in TG-treated cells (Fig. 8B). These results are in agreement with data previously obtained by Lee showing that inhibition of JNK phosphorylation with SP600125 is able to increase $mtO_2^{\bullet -}$ production in cells exposed to DNA damage (Lee et al., 2010).

Finally, in order to determine whether JNK phosphorylation has an impact on the fragmentation of mitochondria in cells exposed to a non-lethal and transient ER stress, we analysed the effect of JNK inhibition in cells exposed to TG or BFA on the morphology of the organelle (Fig. 8C). The quantification of the aspect ratio of mitochondrial network in cells treated with TG or BFA revealed a significant increase in the aspect ratio and thus, a reduced mitochondrial fragmentation, when cells were also incubated with the JNK inhibitor. Altogether, these results show a correlation between the reduced $mtO_2^{\bullet -}$ production and the increased fragmentation of mitochondria and suggest that both biological responses are under the control of activated JNK in HepG2 cells exposed to a transient and non-lethal ER stress.

Discussion

In this study, we demonstrated that a sublethal and transient ER stress provokes the fragmentation of the mitochondrial network accompanied with perturbations of some mitochondrial functions that could be, at least partly, JNK-dependent. Over the past decade, evidence has accumulated demonstrating that the mitochondrial population exhibits functional and morphological changes in response to endoplasmic reticulum stress associated with several chronic diseases such as type 2 diabetes or neurodegenerative diseases (Lindholm et al., 2006; Papa, 2012). However, these few studies were dealing with severe ER stress leading to mitochondrial alterations that trigger apoptosis (Hom et al., 2007; Deniaud et al., 2008; Grimm, 2012). Recent evidence shows that an intimate molecular communication does exist between ER and mitochondria at the MAM contact sites, favoring molecular exchanges under stressing conditions (Arruda et al., 2014; Grimm, 2012). For example, while in the early phase of UPR, calcium buffered by mitochondria seems crucial in the attempt to reestablish calcium homeostasis in the cell during the adaptive ER response, transfer of Ca^{2+} from ER to mitochondria is also essential in inducing mitochondria-dependent cell death in prolonged responses to ER stress (Bravo et al., 2011). UPR^{er} can take place in normal cellular developmental processes that increase the demand for protein folding capacity of the ER as observed for instance during B-lymphocyte differentiation into plasma B-cells that secrete large amounts of immunoglobulins (Gass et al., 2002; Cenci and Sitia, 2007). Pancreatic β-cells, due to insulin synthesis and secretory activity, are also highly exposed and known to be particularly sensitive to ER stress (Laybutt et al., 2007; Song et al., 2008). However, differentiating/or differentiated cells are equipped with stringent checkpoint mechanisms to elicit rapid adaptive responses and face the ER stress by increasing their ER volume and the expression of UPR targets including the ER chaperones BiP and Grp94 as well as the ERAD actors for degradation of unfolded proteins (Calfon et al., 2002; Gass et al., 2002; Iwakoshi et al., 2003).

Besides cell signaling that favors or inhibits adaptive UPR during cell adjustment to a sublethal and transient ER stress, metabolism and more specifically mitochondrial adjustment might also help cells to cope with mild and non-lethal ER stressing conditions. The first line of evidence supporting the participation of mitochondria to this process came from a study showing that mitochondrial metabolism is stimulated during the adaptive phase of the ER stress (Bravo et al., 2011), a phenomenon that depends crucially on physical interactions between ER and mitochondria favoring Ca^{2+} transfer between both organelles (Bravo et al., 2011).

In this study on HepG2 cells, we analyzed the effect of a mild and transient ER stress induced by TG or BFA that does not lead to apoptosis (as assessed by the absence of cleavage of caspase-3, PARP-1, and DNA fragmentation) on the mitochondrial population. We show that, in HepG2 cells incubated with 50 nM TG or 500 nM BFA, the abundance of phospho-eIF2α, phospho-IRE1, and BiP increases evidencing the activation of the three UPR uptstream sensors even if the intensity and time-course of activation are different (Figs. 1 and 2). In addition, the activation of the transcription factor sXBP1 was also observed in cells exposed to TG or BFA (Fig. 1D).

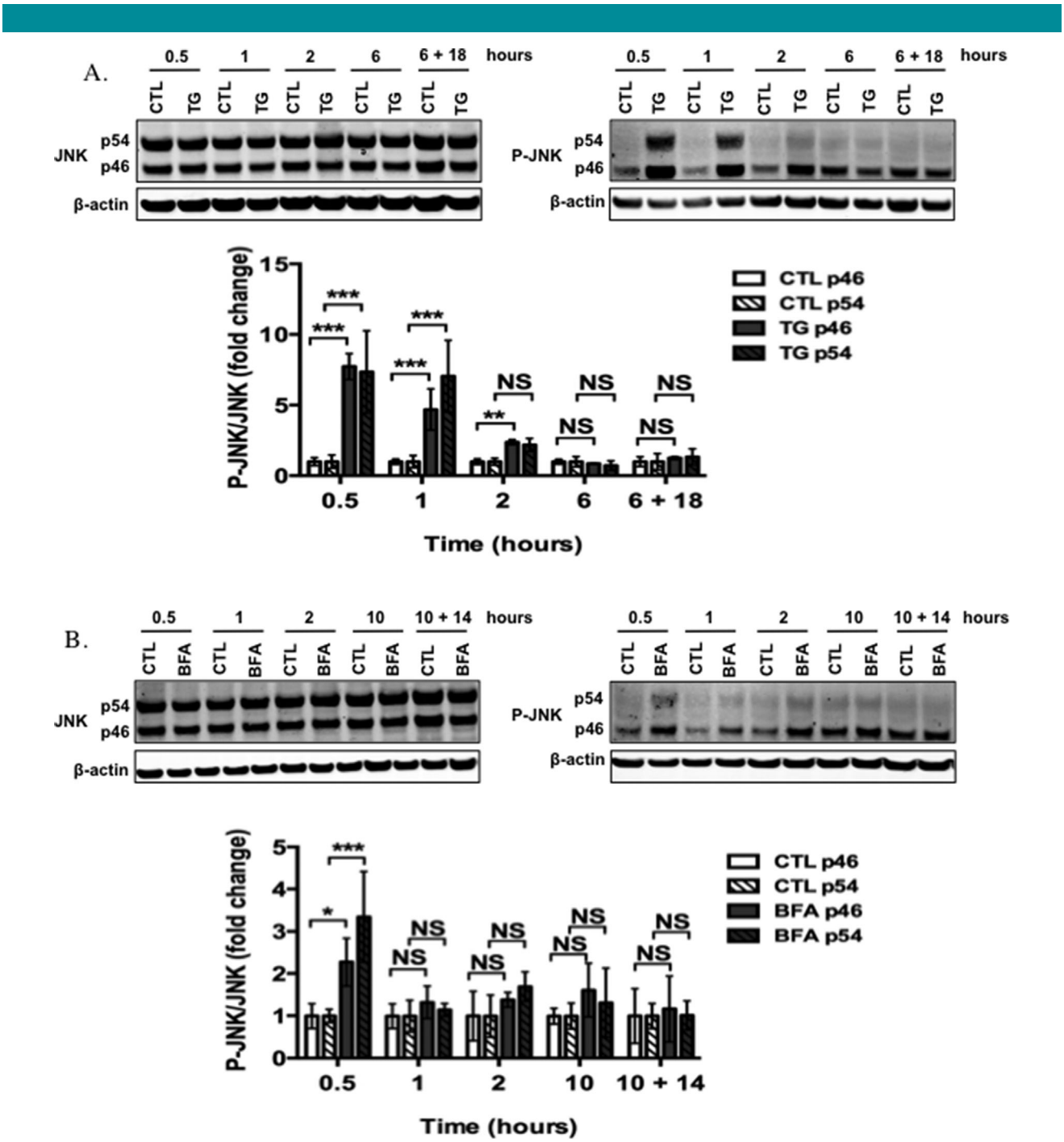

Fig. 7. ER stress-induced phosphorylation of JNK. A: The abundance of the phosphorylated form of JNK was analyzed by Western blot on 15 μg of clear cell lysates prepared from HepG2 cells incubated in presence of 50 nM TG (A) or 500 nM BFA (B) for different incubation times and followed or not by a recovery period. Signal intensity was quantified and normalized to the abundance of β-actin (loading control). Results are expressed in fold change and represent means ± SD (n = 3). NS: not significant; *, **, or *: significantly different from CTL cells with $P < 0.05$; <0.01, <0.001, respectively.**

We next studied the impact of a non-lethal ER stress on mitochondrial bioenergetics (mitochondrial membrane potential, OCR and ATP content) and observed different responses (in terms of magnitude and time-course) to the stress induced by either TG or BFA.

TG, an irreversible inhibitor of the SERCA pumps, is widely used at high concentration (1–5 μM) to study the pathways involved in ER stress-induced apoptosis by a mechanism that would involve either JNK/p38MAPK triggering the subsequent activation of the calpain/caspase-12 pathway (Huang et al., 2014) or apoptosis triggered via a reduction of the mitochondrial membrane potential, an increase in the $mtO_2^{\bullet-}$ production leading to the opening of the MPTP (Deniaud et al., 2008; Zhang et al., 2008).

In this study, HepG2 cells incubated in the presence of TG responded rapidly and strongly by decreasing the

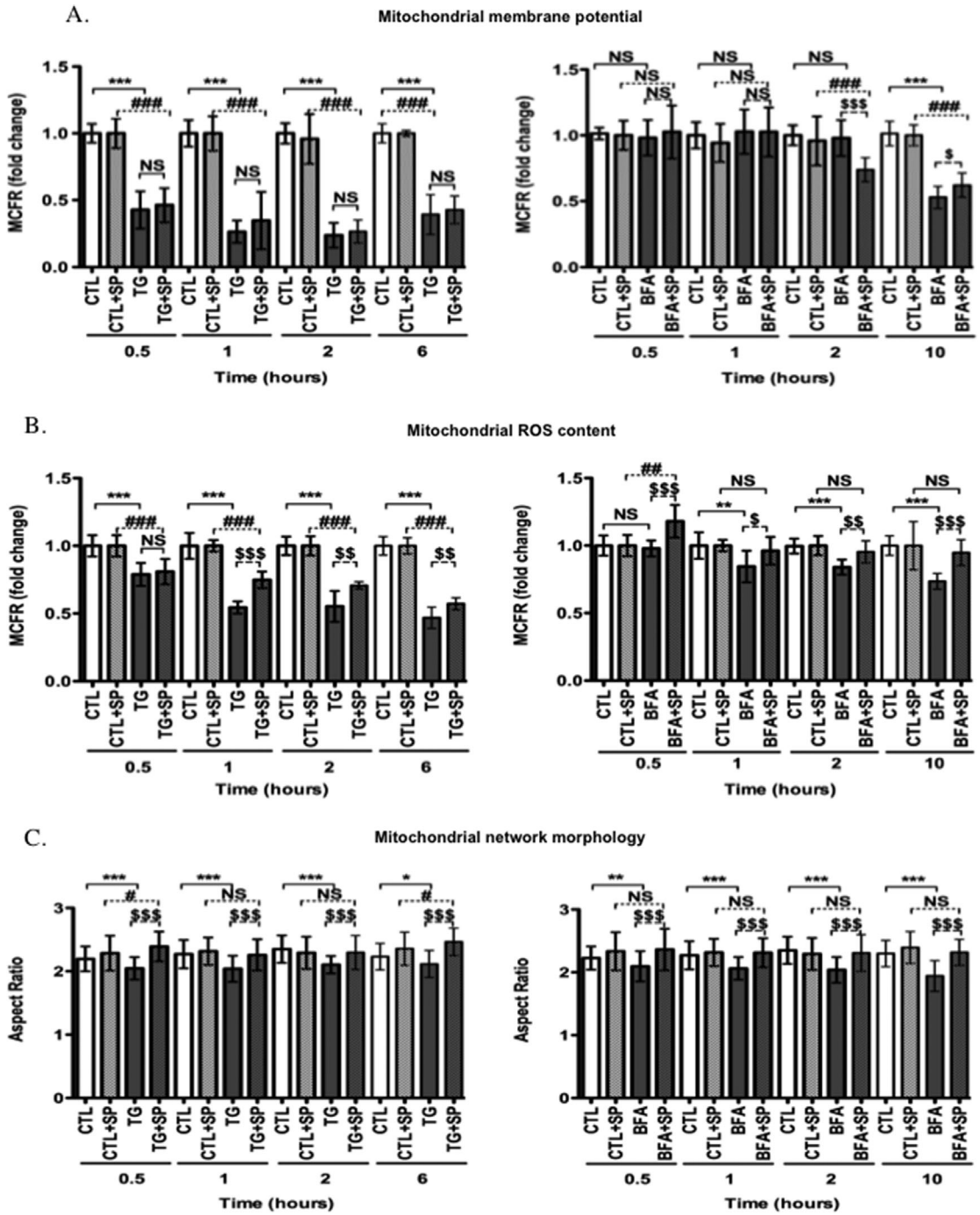

Fig. 8. Inhibition of JNK phosphorylation with SP600125 restores basal functions and morphology of mitochondria after an ER stress. A: The mitochondrial membrane potential was analyzed in HepG2 cells pre-incubated in the presence of 40 μM SP600125 for 1 h and then incubated with 50 nM TG or 500 nM BFA for different period using the mitochondrial membrane potential probe TMRE. Cells were stained or not (to allow auto-fluorescence determination from cells without dye) with 25 nM TMRE for 30 min and fluorescence was analyzed by flow cytometry. Results are expressed as MCFR and are presented as means ± SD (n = 3). NS: not significant; $: significantly different from appropriate CTL cells with $P < 0.05$; *, ###, or $$$: with $P < 0.001$. B: The $mtO_2^{\bullet-}$ content was assessed in HepG2 cells pre-incubated in the presence of 40 μM SP600125 for 1 h and then incubated with 50 nM TG or 500 nM BFA for different periods of time using the mitochondrial MitoSOX™ Red dye. Cells were stained or not with 5 μM MitoSOX™ Red dye for 20 min. Fluorescence was measured by flow cytometry. Results are expressed as fluorescence MCFR and are presented as means ± SD (n = 3). NS: not significant; $: significantly different from appropriate CTL cells with $P < 0.05$; ** or $$: $P < 0.01$ and ***, ###, or $$$: $P < 0.001$. C: The length (or Aspect Ratio, AR) of the mitochondrial fragments was analyzed in HepG2 cells pre-incubated in the presence of 40 μM SP600125 for 1 h and then incubated with 50 nM TG or 500 nM BFA for different periods using the probe Mitotracker Green. The AR was determined on micrographs using the ImageJ 64 software as described in the Materials and Methods section. Results are expressed in Aspect ratio and represent means ± SD (at least 100 events/cell, n ≥ 40 cells from three independent experiments). NS: not significant; * or #: significantly different from appropriate CTL cells with $P < 0.05$; **: $P < 0.01$; *** or $$$: $P < 0.001$.**

mitochondrial membrane potential, reducing the $mtO_2^{\bullet-}$ production and respiration and by increasing the matrix calcium concentration without inducing apoptosis (Figs. 4 and 5). These effects are reversible as they were no longer observed after a recovery period. Indeed, after an 18 h resting period, the basal respiration and the ATP content were increased in TG-treated cells, meaning that cells faced the stress, relying even more on OXPHOS to produce ATP after the stress. BFA exerted milder effects on mitochondrial functions as only a slight decrease in the respiration (assessed by real time OCR) and $mtO_2^{\bullet-}$ production were observed at the early incubation time points. In addition, in BFA-treated cells, while the mitochondrial respiration is slightly increased after a recovery period, it does not have any impact on global ATP content while a TG-treatment does (Fig. 4C). Moreover, not only is the effect of the BFA-induced stress milder but some changes on mitochondrial parameters are delayed as we detected a decrease in mitochondrial membrane potential only in HepG2 cells incubated with BFA for 10 h and after the recovery period (Figs. 4 and 5). Finally, contrary to TG, BFA did not affect the mitochondrial matrix Ca^{2+} concentration (Fig. 5A) (Deniaud et al., 2008).

It is important to emphasize that, in our experimental conditions, we observed a decrease in the mitochondrial membrane potential associated with a decrease in the $mtO_2^{\bullet-}$ detection while in studies using high concentrations of ER stressors triggering apoptosis, a decrease in the mitochondrial membrane potential is usually associated with an increase in ROS production (Choi et al., 2010; Wang and Welsh, 2014).

These observations could be explained by the activation of a mild uncoupling that lowers the mitochondrial membrane potential as a possible strategy for cell adaptation and protection against ROS production and oxidative stress (Murphy, 2009). These authors proposed that an increase in mitochondrial membrane potential (hyperpolarization) would lead to an increase in electron leak from the electron transport chain (ETC) and thus to a higher production of superoxide radical anion and other ROS-derivatives (Murphy, 2009). On the contrary, a mild uncoupling increases the flux of electrons in the ETC as well as the oxygen consumption, leading to a local decrease in oxygen concentration and mitochondrial proton motive force, thus decreasing mitochondrial ROS production. This mechanism could explain how a reduced mitochondrial membrane potential is associated with a lower mitochondrial ROS production (Brand et al., 2004; Mailloux and Harper, 2011). Activation of this mechanism could thus be seen as a protective adjustment against a mild and non lethal ER stress.

Taken together, these results show that a mild and transient ER stress affects several functional parameters of mitochondria keeping the severity and time-course of modifications compatible with cell survival, preventing apoptosis. Because a sustained ER stress can induce apoptosis and because apoptosis is often accompanied by morphological changes of the mitochondrial network such as fragmentation (Breckenridge et al., 2003; Hom et al., 2007), we measured the reticulation status of the mitochondrial network in HepG2 exposed to a mild ER stress (Fig. 3A and B) and indeed observed a rapid fragmentation of the network in cells exposed to either TG or BFA.

To unravel the underlying mechanisms in this mitochondrial fragmentation, we assessed the abundance of the actors involved in the regulation of mitochondrial morphology. So far, in eukaryotes, several proteins have been identified as regulating those events. Among them, Mfn1 and Mfn2 are two GTPases involved in the fusion of the OMM (Koshiba et al., 2004). Fusion of the IMM and maintenance of the cristae is ensured by the Opa1 GTPase (Song et al., 2009; Mishra et al., 2014). Mitochondrial fission in mammals is mainly mediated by Drp1, a cytosolic GTPase that can be recruited to the OMM and potentially binds to four mitochondrial receptor proteins: Fis 1, MFF, MiD49, and MiD51 (Loson et al., 2013; Palmer et al., 2013). We first checked the abundance of all these actors in total cell extracts (Fig. 6 and Supporting Information Fig. S4) or in mitochondria-enriched fractions (Supporting Information Fig. S7), but we could not see any changes in samples prepared from cells incubated with TG (Fig. 6A and Supporting Information Fig. S4A) or BFA (Supporting Information Fig. S4B), except a strong increase in the abundance of Fis1 in BFA-treated cells after a 14 h of recovery (Fig. 6B and C). Because Fis1 could recruit Drp1 to trigger mitochondrial fission, we also analyzed the co-localization of these two proteins in cells incubated in presence of BFA (Supporting Information Fig. S5A and B) but no change in the recruitment of Drp1 by Fis1 was observed. Moreover, it is unlikely that the increased expression of Fis1 plays a significant role in mitochondrial fragmentation observed in cells exposed to mild ER stress as silencing of Fis1 (Supporting Information Fig. S6B and C) did not reverse the mitochondrial fragmentation observed in BFA- or TG-treated cells. We, therefore, focused our attention on some putative post-translational mechanisms involved in fragmentation known to be independent on changes in the abundance of the mitochondrial dynamics actors. Indeed, besides its role in mitochondrial fusion, Mfn2 is also present at the contact points between ER and mitochondria (de Brito and Scorrano, 2008; Garcia-Perez et al., 2011). We hypothesized that a mislocalization of this protein would weaken, at least partially, the physical interactions between ER and mitochondria, disturbing the communication between the two organelles, leading to mitochondrial dysfunction. Mfn2 is known to be K63-polyubiquitinylated by MITOL, a mitochondrial ubiquitin ligase (Sugiura et al., 2013). This non-degradative polyubiquitinylation regulates the formation of mitochondria-ER bridges at the MAM junctions (Sugiura et al., 2013). We thus performed immunoprecipitations of Mfn2 on mitochondria-enriched fractions from cells incubated or not with BFA and observed the presence of K63-linked polyubiquitin chains coupled to Mfn2. However, no change in the abundance of these K63-linked polyubiquitin chains was observed in BFA-treated cells when compared with control cells (data not shown).

Several signaling mechanisms have been linked to ER stress (Vannuvel et al., 2013), among which IRE1, not only as a dual enzyme, but also as a platform leading to the sequential activation of the TRAF2-ASK1-JNK pathway, resulting in the activation of transcription factors such as CHOP or p53 that up-regulate the expression of genes actively involved in cell death such as *Bim* (Zheng et al., 2013; Jiang et al., 2015). A recent study demonstrated that, in hepatocytes and HeLa cells, tunicamycin or BFA-induced ER stress activates the IRE1-JNK pathway leading to the phosphorylation of JNK and subsequent interaction with Sab (SH3 homology associated BTK binding protein) at the OMM, a key event in the perturbation of mitochondrial respiration and in cell death induced by ER stress (Win et al., 2014). We found that JNK is strongly and rapidly (but transiently) phosphorylated in TG-treated cells (Fig. 7A). JNK phosphorylation in BFA-treated cells is also slightly increased after a 30 min incubation (Fig. 7B). We next showed that when JNK was inhibited in the presence of SP600125, mitochondrial fragmentation was not observed anymore and the signals for $mtO_2^{\bullet-}$ detection was less reduced in both BFA- and TG-treated cells even if the inhibitor had no effect on the mitochondrial membrane potential (Fig. 8A–C). These results demonstrate that changes induced in mitochondrial morphology after a mild and non lethal ER stress are not reducing the ATP content and are mediated, at least partly, by the subsequent activation of JNK. Even if activation of JNK is known to be mainly pro-apoptotic (Verma and Datta, 2012; Huang et al., 2014; Win et al., 2015), several studies

demonstrated that the activation of JNK could also be pro-survival (Yang and Chan, 2009; Lee et al., 2010). Indeed, JNK phosphorylates several substrates in response to different stresses such as Bcl-2 on Ser70, a post-translational modification that is required for its full and potent anti-apoptotic activity (Ito et al., 1997; Deng et al., 2001). Moreover, Bcl-2 phosphorylation on Ser70 by JNK has a critical role in maintaining cell cycle progression and in preventing premature senescence in MCF7 breast carcinoma cells (Lee et al., 2010). More recently, studies also demonstrated that ER-mitochondria contact sites act as a platform providing the membranes for the autophagosomes involved in autophagy (Betz et al., 2013; Hamasaki et al., 2013). Indeed, accumulating evidence suggests that ER stress triggers autophagy which may determine cell fate by protecting cells from destruction or by inducing cell death (Shi et al., 2011; Su et al., 2013). A recent study demonstrated that ER stress induced with tunicamycin in breast cancer cells triggers the IRE1-JNK-Beclin1 pathway which attenuates ER stress by clearing ubiquitinylated proteins and decreasing apoptosis (Cheng et al., 2014). Altogether, these studies suggest that cells could trigger a pro-survival autophagy mechanism at the ER-mitochondria contact points to deal with the activation of the UPR after an ER stress.

In summary, we demonstrated that TG or BFA, two specific chemical inducers used at low concentrations, mimicking a mild and transient ER stress in HepG2 cells, caused a rapid alteration of mitochondrial morphology and of several mitochondrial functions that do not necessarily affect the global ATP content. Some of these modifications are, at least partially, dependent on transient JNK phosphorylation. Future work should determine whether the activation of JNK is pro-survival, a process that could rely on either Bcl-2 phosphorylation at Ser70 or on the activation of pro-survival autophagy. In this study, we thus characterized a potential signaling pathway potentially involved in physiological ER stress compatible with cell survival, a condition still poorly studied when compared with pro-apoptotic ER stress usually characterized by intense and prolonged ER stress. In the future, this signaling pathway should also be studied in more relevant biological systems and conditions in which adaptive responses are expected such as in pancreatic β-cells producing high amounts of insulin to meet demands in response to insulin resistance or in cell survival mechanisms allowing plasma B-cells to produce high amount of antibodies in response to infection.

Acknowledgements

The authors thank the researchers from the group of Pr. Sonveaux and particularly Paolo Porporato (FATH, IREC, Université Catholique de Louvain, Brussels, Belgium) for their help with respiration analyses. This work was supported by the Belgian Association for Muscular Diseases (ABMM, Belgium, grant 2013-08) and the University of Namur, Belgium. The immunofluorescence staining observation with confocal microscopy and calcium measurements using the BD Pathway 855 were performed using the "morphology" technological platform (University of Namur). The confocal microscopy and the BD Pathway 855 were acquired with a grant from the Fonds de la Recherche Scientifique (F.R.S-FNRS; grant no. 2.5008.11).

Literature Cited

Arruda AP, Pers BM, Parlakgul G, Guney E, Inouye K, Hotamisligil GS. 2014. Chronic enrichment of hepatic endoplasmic reticulum-mitochondria contact leads to mitochondrial dysfunction in obesity. Nat Med 20:1427–1435.

Baumann O, Walz B. 2001. Endoplasmic reticulum of animal cells and its organization into structural and functional domains. Int Rev Cytol 205:149–214.

Baumgartner HK, Gerasimenko JV, Thorne C, Ferdek P, Pozzan T, Tepikin AV, Petersen OH, Sutton R, Watson AJ, Gerasimenko OV. 2009. Calcium elevation in mitochondria is the main Ca2+ requirement for mitochondrial permeability transition pore (mPTP) opening. J Biol Chem 284:20796–20803.

Benyair R, Ron E, Lederkremer GZ. 2011. Protein quality control, retention, and degradation at the endoplasmic reticulum. Int Rev Cell Mol Biol 292:197–280.

Berridge MJ. 2002. The endoplasmic reticulum: A multifunctional signaling organelle. Cell Calcium 32:235–249.

Bertolotti A, Zhang Y, Hendershot LM, Harding HP, Ron D. 2000. Dynamic interaction of BiP and ER stress transducers in the unfolded-protein response. Nat Cell Biol 2:326–332.

Betz C, Stracka D, Prescianotto-Baschong C, Frieden M, Demaurex N, Hall MN. 2013. Feature Article: mTOR complex 2-Akt signaling at mitochondria-associated endoplasmic reticulum membranes (MAM) regulates mitochondrial physiology. Proc Natl Acad Sci USA 110:12526–12534.

Bogoyevitch MA, Arthur PG. 2008. Inhibitors of c-Jun N-terminal kinases: JuNK no more? Biochi Biophys Acta 1784:76–93.

Brand MD, Affourtit C, Esteves TC, Green K, Lambert AJ, Miwa S, Pakay JL, Parker N. 2004. Mitochondrial superoxide: Production, biological effects, and activation of uncoupling proteins. Free Rad Biol Med 37:755–767.

Brand MD, Nicholls DG. 2011. Assessing mitochondrial dysfunction in cells. Biochem J 435:297–312.

Bras M, Queenan B, Susin SA. 2005. Programmed cell death via mitochondria: Different modes of dying. Biochemistry 70:231–239.

Bravo R, Vicencio JM, Parra V, Troncoso R, Munoz JP, Bui M, Quiroga C, Rodriguez AE, Verdejo HE, Ferreira J, Iglewski M, Chiong M, Simmen T, Zorzano A, Hill JA, Rothermel BA, Szabadkai G, Lavandero S. 2011. Increased ER-mitochondrial coupling promotes mitochondrial respiration and bioenergetics during early phases of ER stress. J Cell Sci 124:2143–2152.

Breckenridge DG, Stojanovic M, Marcellus RC, Shore GC. 2003. Caspase cleavage product of BAP31 induces mitochondrial fission through endoplasmic reticulum calcium signals, enhancing cytochrome c release to the cytosol. J Cell Biol 160:1115–1127.

Brewer JW. 2014. Regulatory crosstalk within the mammalian unfolded protein response. Cell Mol Life Sci 71:1067–1079.

Burte F, Carelli V, Chinnery PF, Yu-Wai-Man P. 2015. Disturbed mitochondrial dynamics and neurodegenerative disorders. Nat Rev Neurol 11:11–24.

Caldeira da Silva CC, Cerqueira FM, Barbosa LF, Medeiros MH, Kowaltowski AJ. 2008. Mild mitochondrial uncoupling in mice affects energy metabolism, redox balance and longevity. Aging Cell 7:552–560.

Calfon M, Zeng H, Urano F, Till JH, Hubbard SR, Harding HP, Clark SG, Ron D. 2002. IRE1 couples endoplasmic reticulum load to secretory capacity by processing the XBP-1 mRNA. Nature 415:92–96.

Cenci S, Sitia R. 2007. Managing and exploiting stress in the antibody factory. FEBS Lett 581:3652–3657.

Cereghetti GM, Stangherlin A, Martins de Brito O, Chang CR, Blackstone C, Bernardi P, Scorrano L. 2008. Dephosphorylation by calcineurin regulates translocation of Drp1 to mitochondria. Proc Natl Acad Sci USA 105:15803–15808.

Chang CR, Blackstone C. 2007. Cyclic AMP-dependent protein kinase phosphorylation of Drp1 regulates its GTPase activity and mitochondrial morphology. J Biol Chem 282:21583–21587.

Chen Q, Vazquez EJ, Moghaddas S, Hoppel CL, Lesnefsky EJ. 2003. Production of reactive oxygen species by mitochondria: Central role of complex III. J Biol Chem 278:36027–36031.

Cheng X, Liu H, Jiang CC, Fang L, Chen C, Zhang XD, Jiang ZW. 2014. Connecting endoplasmic reticulum stress to autophagy through IRE1/JNK/beclin-1 in breast cancer cells. Int J Mol Med 34:772–781.

Cho B, Cho HM, Kim HJ, Jeong J, Park SK, Hwang EM, Park JY, Kim WR, Kim H, Sun W. 2014. CDK5-dependent inhibitory phosphorylation of Drp1 during neuronal maturation. Exp Mol Med 46:e105.

Choi JH, Choi AY, Yoon H, Choe W, Yoon KS, Ha J, Yeo EJ, Kang I, . 2010. Baicalein protects HT22 murine hippocampal neuronal cells against endoplasmic reticulum stress-induced apoptosis through inhibition of reactive oxygen species production and CHOP induction. Exp Mol Med 42:811–822.

Cosentino K, Garcia-Saez AJ. 2014. Mitochondrial alterations in apoptosis. Chem Phys Lipid 181:62–75.

de Brito OM, Scorrano L. 2008. Mitofusin 2 tethers endoplasmic reticulum to mitochondria. Nature 456:605–610.

de la Cadena SG, Hernandez-Fonseca K, Camacho-Arroyo I, Massieu L. 2014. Glucose deprivation induces reticulum stress by the PERK pathway and caspase-7- and calpain-mediated caspase-12 activation. Apoptosis 19:414–427.

de Longueville F, Atienzar FA, Marcq L, Dufrane S, Evrard S, Wouters L, Leroux F, Bertholet V, Gerin B, Whomsley R, Arnould T, Remacle J, Canning M. 2003. Use of a low-density microarray for studying gene expression patterns induced by hepatotoxicants on primary cultures of rat hepatocytes. Toxicol Sci 75:378–392.

De Vos KJ, Sheetz MP. 2007. Visualization and quantification of mitochondrial dynamics in living animal cells. Methods Cell Biol 80:627–682.

Delic M, Rebnegger C, Wanka F, Puxbaum V, Haberhauer-Troyer C, Hann S, Kollensperger G, Mattanovich D, Gasser B. 2012. Oxidative protein folding and unfolded protein response elicit differing redox regulation in endoplasmic reticulum and cytosol of yeast. Free Rad Biol Med 52:2000–2012.

Deng X, Xiao L, Lang W, Gao F, Ruvolo P, May WS, Jr. 2001. Novel role for JNK as a stress-activated Bcl2 kinase. J Biol Chem 276:23681–23688.

Deniaud A, Sharaf el dein O, Maillier E, Poncet D, Kroemer G, Lemaire C, Brenner C. 2008. Endoplasmic reticulum stress induces calcium-dependent permeability transition, mitochondrial outer membrane permeabilization and apoptosis. Oncogene 27:285–299.

Duchen MR. 2004. Mitochondria in health and disease: Perspectives on a new mitochondrial biology. Mol Aspects Med 25:365–451.

Dufey E, Sepulveda D, Rojas-Rivera D, Hetz C. 2014. Cellular mechanisms of endoplasmic reticulum stress signaling in health and disease. 1. An overview. Am J Physiol Cell Phys 307: C582–C594.

DuRose JB, Tam AB, Niwa M. 2006. Intrinsic capacities of molecular sensors of the unfolded protein response to sense alternate forms of endoplasmic reticulum stress. Mol Biol Cell 17:3095–3107.

Eom KS, Kim HJ, So HS, Park R, Kim TY. 2010. Berberine-induced apoptosis in human glioblastoma T98G cells is mediated by endoplasmic reticulum stress accompanying reactive oxygen species and mitochondrial dysfunction. Biol Pharm Bull 33:1644–1649.

Foldi I, Toth AM, Szabo Z, Mozes E, Berkecz R, Datki ZL, Penke B, Janaky T. 2013. Proteome-wide study of endoplasmic reticulum stress induced by thapsigargin in N2a neuroblastoma cells. Neurochem Int 62:58–69.

Friedman JR, Lackner LL, West M, DiBenedetto JR, Nunnari J, Voeltz GK. 2011. ER tubules mark sites of mitochondrial division. Science 334:358–362.
Fu S, Watkins SM, Hotamisligil GS. 2012. The role of endoplasmic reticulum in hepatic lipid homeostasis and stress signaling. Cell Metabol 15:623–634.
Fu Y, Li J, Lee AS. 2007. GRP78/BiP inhibits endoplasmic reticulum BIK and protects human breast cancer cells against estrogen starvation-induced apoptosis. Cancer Res 67:3734–3740.
Fujiwara T, Oda K, Yokota S, Takatsuki A, Ikehara Y. 1988. Brefeldin A causes disassembly of the Golgi complex and accumulation of secretory proteins in the endoplasmic reticulum. J Biol Chem 263:18545–18552.
Galloway CA, Yoon Y. 2013. Mitochondrial morphology in metabolic diseases. Antioxi Redox Signal 19:415–430.
Garcia-Perez C, Schneider TG, Hajnoczky G, Csordas G. 2011. Alignment of sarcoplasmic reticulum-mitochondrial junctions with mitochondrial contact points. Am J Physiol Heart Circul Phys 301:H1907–H1915.
Gass JN, Gifford NM, Brewer JW. 2002. Activation of an unfolded protein response during differentiation of antibody-secreting B cells. J Biol Chem 277:49047–49054.
Gingrich JC, Davis DR, Nguyen Q. 2000. Multiplex detection and quantitation of proteins on western blots using fluorescent probes. BioTechniques 29:636–642.
Grimm S. 2012. The ER-mitochondria interface: The social network of cell death. Biochim Biophys Acta 1823:327–334.
Groenendyk J, Michalak M. 2005. Endoplasmic reticulum quality control and apoptosis. Acta Biochim Pol 52:381–395.
Guimaraes EL, Best J, Dolle L, Najimi M, Sokal E, van Grunsven LA. 2012. Mitochondrial uncouplers inhibit hepatic stellate cell activation. BMC Gastroenterol 12:68.
Hamasaki M, Furuta N, Matsuda A, Nezu A, Yamamoto A, Fujita N, Oomori H, Noda T, Haraguchi T, Hiraoka Y, Amano A, Yoshimori T. 2013. Autophagosomes form at ER-mitochondria contact sites. Nature 495:389–393.
Hamman BD, Hendershot LM, Johnson AE. 1998. BiP maintains the permeability barrier of the ER membrane by sealing the lumenal end of the translocon pore before and early in translocation. Cell 92:747–758.
Hetz C. 2012. The unfolded protein response: Controlling cell fate decisions under ER stress and beyond. Nat Rev Mol Cell Biol 13:89–102.
Hom JR, Gewandter JS, Michael L, Sheu SS, Yoon Y. 2007. Thapsigargin induces biphasic fragmentation of mitochondria through calcium-mediated mitochondrial fission and apoptosis. J Cell Phys 212:498–508.
Huang Y, Li X, Wang Y, Wang H, Huang C, Li J. 2014. Endoplasmic reticulum stress-induced hepatic stellate cell apoptosis through calcium-mediated JNK/P38 MAPK and Calpain/Caspase-12 pathways. Mol Cell Biochem 394:1–12.
Iqbal S, Hood DA. 2014. Oxidative stress-induced mitochondrial fragmentation and movement in skeletal muscle myoblasts. Am J Physiol Cell Physiol 306:C1176–C1183.
Iqbal S, Hood DA. 2015. The role of mitochondrial fusion and fission in skeletal muscle function and dysfunction. Front Biosci 20:157–172.
Ito T, Deng X, Carr B, May WS. 1997. Bcl-2 phosphorylation required for anti-apoptosis function. J Biol Chem 272:11671–11673.
Iwakoshi NN, Lee AH, Vallabhajosyula P, Otipoby KL, Rajewsky K, Glimcher LH. 2003. Plasma cell differentiation and the unfolded protein response intersect at the transcription factor XBP-1. Nat Immunol 4:321–329.
Iwawaki T, Oikawa D. 2013. The role of the unfolded protein response in diabetes mellitus. Semin Immunopathol 35:333–350.
Jiang Q, Yuan Y, Zhou J, Wu Y, Zhou Q, Gui S, Wang Y. 2015. Apoptotic events induced by high glucose in human hepatoma HepG2 cells involve endoplasmic reticulum stress and MAPK's activation. Mol Cell Biochem 399:113–122.
Joshi DC, Bakowska JC. 2011. Determination of mitochondrial membrane potential and reactive oxygen species in live rat cortical neurons. J Vis Exp May 23;(51). pii: 2704. doi: 10.3791/2704
Karbowski M, Arnoult D, Chen H, Chan DC, Smith CL, Youle RJ. 2004. Quantitation of mitochondrial dynamics by photolabeling of individual organelles shows that mitochondrial fusion is blocked during the Bax activation phase of apoptosis. J Cell Biol 164:493–499.
Koshiba T, Detmer SA, Kaiser JT, Chen H, McCaffery JM, Chan DC. 2004. Structural basis of mitochondrial tethering by mitofusin complexes. Science 305:858–862.
Kucharz K, Wieloch T, Toresson H. 2013. Fission and fusion of the neuronal endoplasmic reticulum. Trans Stroke Res 4:652–662.
Lackner LL. 2014. Shaping the dynamic mitochondrial network. BMC Biol 12:35.
Landau G, Kodali VK, Malhotra JD, Kaufman RJ. 2013. Detection of oxidative damage in response to protein misfolding in the endoplasmic reticulum. Methods Enzymol 526:231–250.
Laybutt DR, Preston AM, Akerfeldt MC, Kench JG, Busch AK, Biankin AV, Biden TJ. 2007. Endoplasmic reticulum stress contributes to beta cell apoptosis in type 2 diabetes. Diabetologia 50:752–763.
Lee J, Ozcan U. 2014. Unfolded protein response signaling and metabolic diseases. J Biol Chem 289:1203–1211.
Lee JJ, Lee JH, Ko YG, Hong SI, Lee JS. 2010. Prevention of premature senescence requires JNK regulation of Bcl-2 and reactive oxygen species. Oncogene 29:561–575.
Lee JS, Mendez R, Heng HH, Yang ZQ, Zhang K. 2012. Pharmacological ER stress promotes hepatic lipogenesis and lipid droplet formation. Am J Trans Res 4:102–113.
Lewis B, Rathman S, McMahon RJ. 2003. Detection and quantification of biotinylated proteins using the Storm 840 Optical Scanner. J Nutr Biochem 14:196–202.
Li H, Korennykh AV, Behrman SL, Walter P. 2010. Mammalian endoplasmic reticulum stress sensor IRE1 signals by dynamic clustering. Proc Natl Acad Sci USA 107:16113–16118.
Lin JH, Li H, Yasumura D, Cohen HR, Zhang C, Panning B, Shokat KM, Lavail MM, Walter P. 2007. IRE1 signaling affects cell fate during the unfolded protein response. Science 318:944–949.
Lindholm D, Wootz H, Korhonen L. 2006. ER stress and neurodegenerative diseases. Cell Death Differ 13:385–392.
Loson OC, Song Z, Chen H, Chan DC. 2013. Fis1, Mff, MiD49, and MiD51 mediate Drp1 recruitment in mitochondrial fission. Mol Biol Cell 24:659–667.
Luvisetto S, Pietrobon D, Azzone GF. 1987. Uncoupling of oxidative phosphorylation. 1. Protonophoric effects account only partially for uncoupling. Biochemistry 26:7332–7338.
Lytton J, Westlin M, Hanley MR. 1991. Thapsigargin inhibits the sarcoplasmic or endoplasmic reticulum Ca-ATPase family of calcium pumps. J Biol Chem 266:17067–17071.
Ma K, Vattem KM, Wek RC. 2002. Dimerization and release of molecular chaperone inhibition facilitate activation of eukaryotic initiation factor-2 kinase in response to endoplasmic reticulum stress. J Biol Chem 277:18728–18735.
Mailloux RJ, Harper ME. 2011. Uncoupling proteins and the control of mitochondrial reactive oxygen species production. Free Rad Biol Med 51:1106–1115.
Marchi S, Patergnani S, Pinton P. 2014. The endoplasmic reticulum-mitochondria connection: One touch, multiple functions. Biochim Biophys Acta 1837:461–469.
Mishra P, Carelli V, Manfredi G, Chan DC. 2014. Proteolytic cleavage of Opa1 stimulates mitochondrial inner membrane fusion and couples fusion to oxidative phosphorylation. Cell Metabol 19:630–641.
Mishra P, Chan DC. 2014. Mitochondrial dynamics and inheritance during cell division, development and disease. Nat Rev Mol Cell Biol 15:634–646.
Moon JL, Kim SY, Shin SW, Park JW. 2012. Regulation of brefeldin A-induced ER stress and apoptosis by mitochondrial NADP(+)-dependent isocitrate dehydrogenase. Biochem Biophys Res Commun 417:760–764.
Mortiboys H, Thomas KJ, Koopman WJ, Klaffke S, Abou-Sleiman P, Olpin S, Wood NW, Willems PH, Smeitink JA, Cookson MR, Bandmann O. 2008. Mitochondrial function and morphology are impaired in parkin-mutant fibroblasts. Annal Neurol 64:555–565.
Murphy MP. 2009. How mitochondria produce reactive oxygen species. Biochem J 417:1–13.
Ohta K, Okayama S, Togo A, Nakamura K. 2014. Three-dimensional organization of the endoplasmic reticulum membrane around the mitochondrial constriction site in mammalian cells revealed by using focused-ion beam tomography. Microscopy 63:34.
Otera H, Wang C, Cleland MM, Setoguchi K, Yokota S, Youle RJ, Mihara K. 2010. Mff is an essential factor for mitochondrial recruitment of Drp1 during mitochondrial fission in mammalian cells. J Cell Biol 191:1141–1158.
Palmer CS, Elgass KD, Parton RG, Osellame LD, Stojanovski D, Ryan MT. 2013. Adaptor proteins MiD49 and MiD51 can act independently of Mff and Fis1 in Drp1 recruitment and are specific for mitochondrial fission. J Biol Chem 288:27584–27593.
Papa FR. 2012. Endoplasmic reticulum stress, pancreatic beta-cell degeneration, and diabetes. Cold Spring Harb Perspect Med 2:a007666.
Pendergrass W, Wolf N, Poot M. 2004. Efficacy of MitoTracker Green and CMXrosamine to measure changes in mitochondrial membrane potentials in living cells and tissues. Cytometry A 61:162–169.
Pineau L, Colas J, Dupont S, Beney L, Fleurat-Lessard P, Berjeaud JM, Berges T, Ferreira T. 2009. Lipid-induced ER stress: Synergistic effects of sterols and saturated fatty acids. Traffic 10:673–690.
Pletjushkina OY, Lyamzaev KG, Popova EN, Nepryakhina OK, Ivanova OY, Domnina LV, Chernyak BV, Skulachev VP. 2006. Effect of oxidative stress on dynamics of mitochondrial reticulum. Biochim Biophy Acta 1757:518–524.
Prostko CR, Brostrom MA, Brostrom CO. 1993. Reversible phosphorylation of eukaryotic initiation factor 2 alpha in response to endoplasmic reticular signaling. Mol Cell Biochem 127-128:255–265.
Qi X, Disatnik MH, Shen N, Sobel RA, Mochly-Rosen D. 2011. Aberrant mitochondrial fission in neurons induced by protein kinase C{delta} under oxidative stress conditions in vivo. Mol Biol Cell 22:256–265.
Regula KM, Ens K, Kirshenbaum LA. 2003. Mitochondria-assisted cell suicide: A license to kill. J Mol Cell Cardiol 35:559–567.
Roy M, Reddy PH, Iijima M, Sesaki H. 2015. Mitochondrial division and fusion in metabolism. Curr Opin Cell Biol 33C:111–118.
Sammels E, Parys JB, Missiaen L, De Smedt H, Bultynck G. 2010. Intracellular Ca2+ storage in health and disease: A dynamic equilibrium. Cell Calcium 47:297–314.
Shen J, Prywes R. 2004. Dependence of site-2 protease cleavage of ATF6 on prior site-1 protease digestion is determined by the size of the luminal domain of ATF6. J Biol Chem 279:43046–43051.
Shi YH, Ding ZB, Zhou J, Hui B, Shi GM, Ke AW, Wang XY, Dai Z, Peng YF, Gu CY, Qiu SJ, Fan J. 2011. Targeting autophagy enhances sorafenib lethality for hepatocellular carcinoma via ER stress-related apoptosis. Autophagy 7:1159–1172.
Slomiany A, Grabska M, Slomiany BA, Grzelinska E, Morita M, Slomiany BL. 1993. Intracellular transport, organelle biogenesis and establishment of Golgi identity: Impact of brefeldin A on the activity of lipid synthesizing enzymes. Int J Biochem 25:891–901.
Snapp EL. 2012. Unfolded protein responses with or without unfolded proteins? Cells 1:926–950.
Song B, Scheuner D, Ron D, Pennathur S, Kaufman RJ. 2008. Chop deletion reduces oxidative stress, improves beta cell function, and promotes cell survival in multiple mouse models of diabetes. J Clin Invest 118:3378–3389.
Song Z, Ghochani M, McCaffery JM, Frey TG, Chan DC. 2009. Mitofusins and OPA1 mediate sequential steps in mitochondrial membrane fusion. Mol Biol Cell 20:3525–3532.
Strack S, Wilson TJ, Cribbs JT. 2013. Cyclin-dependent kinases regulate splice-specific targeting of dynamin-related protein 1 to microtubules. J Cell Biol 201:1037–1051.
Su J, Zhou L, Kong X, Yang X, Xiang X, Zhang Y, Li X, Sun L. 2013. Endoplasmic reticulum is at the crossroads of autophagy, inflammation, and apoptosis signaling pathways and participates in the pathogenesis of diabetes mellitus. J Diabetes Res 2013:193461.
Sugiura A, Nagashima S, Tokuyama T, Amo T, Matsuki Y, Ishido S, Kudo Y, McBride HM, Fukuda T, Matsushita N, Inatome R, Yanagi S. 2013. MITOL regulates endoplasmic reticulum-mitochondria contacts via Mitofusin2. Mol Cell 51:20–34.
Sun J, Cui J, He Q, Chen Z, Arvan P, Liu M. 2015. Proinsulin misfolding and endoplasmic reticulum stress during the development and progression of diabetes. Mol Aspect Med 42:105–118.
Urra H, Dufey E, Lisbona F, Rojas-Rivera D, Hetz C. 2013. When ER stress reaches a dead end. Biochim Biophys Acta 1833:3507–3517.
Vance JE. 2014. MAM (mitochondria-associated membranes) in mammalian cells: Lipids and beyond. Biochim Biophys Acta 1841:595–609.
Vannuvel K, Renard P, Raes M, Arnould T. 2013. Functional and morphological impact of ER stress on mitochondria. J Cell Physiol 228:1802–1818.
Verma G, Datta M. 2012. The critical role of JNK in the ER-mitochondrial crosstalk during apoptotic cell death. J Cell Physiol 227:1791–1795.
Wakabayashi S, Yoshida H. 2013. The essential biology of the endoplasmic reticulum stress response for structural and computational biologists. Comput Struct Biotechnol J 6:e201303010.
Walter F, Schmid J, Dussmann H, Concannon CG, Prehn JH. 2015. Imaging of single cell responses to ER stress indicates that the relative dynamics of IRE1/XBP1 and PERK/ATF4 signalling rather than a switch between signalling branches determine cell survival. Cell Death Diff 22:1502–1516.
Walter P, Ron D. 2011. The unfolded protein response: From stress pathway to homeostatic regulation. Science 334:1081–1086.
Wanet A, Remacle N, Najar M, Sokal E, Arnould T, Najimi M, Renard P. 2014. Mitochondrial remodeling in hepatic differentiation and dedifferentiation. Int J Biochem Cell Biol 54:174–185.
Wang S, Kaufman RJ. 2014. How does protein misfolding in the endoplasmic reticulum affect lipid metabolism in the liver? Curr Opin Lipidol 25:125–132.
Wang X, Welsh N. 2014. Bcl-2 maintains the mitochondrial membrane potential, but fails to affect production of reactive oxygen species and endoplasmic reticulum stress, in sodium palmitate-induced beta-cell death. Ups J Med Sci 119:306–315.

Westrate LM, Lee JE, Prinz WA, Voeltz GK. 2015. Form follows function: The importance of endoplasmic reticulum shape. Annu Rev Biochem 84:791–811.
Win S, Than TA, Fernandez-Checa JC, Kaplowitz N. 2014. JNK interaction with Sab mediates ER stress induced inhibition of mitochondrial respiration and cell death. Cell Death Dis 5:e989.
Win S, Than TA, Le BH, Garcia-Ruiz C, Fernandez-Checa JC, Kaplowitz N. 2015. Sab (Sh3bp5) dependence of JNK mediated inhibition of mitochondrial respiration in palmitic acid induced hepatocyte lipotoxicity. J Hepatol 62:1367–1374.
Yang X, Chan C. 2009. Repression of PKR mediates palmitate-induced apoptosis in HepG2 cells through regulation of Bcl-2. Cell Res 19:469–486.
Yen YP, Tsai KS, Chen YW, Huang CF, Yang RS, Liu SH. 2012. Arsenic induces apoptosis in myoblasts through a reactive oxygen species-induced endoplasmic reticulum stress and mitochondrial dysfunction pathway. Arch Toxicol 86:923–933.
Yoshida H, Matsui T, Yamamoto A, Okada T, Mori K. 2001. XBP1 mRNA is induced by ATF6 and spliced by IRE1 in response to ER stress to produce a highly active transcription factor. Cell 107:881–891.
Yu T, Fox RJ, Burwell LS, Yoon Y. 2005. Regulation of mitochondrial fission and apoptosis by the mitochondrial outer membrane protein hFis1. J Cell Sci 118:4141–4151.
Yu T, Jhun BS, Yoon Y. 2011. High-glucose stimulation increases reactive oxygen species production through the calcium and mitogen-activated protein kinase-mediated activation of mitochondrial fission. Antiox Redox Signal 14:425–437.
Zhang D, Lu C, Whiteman M, Chance B, Armstrong JS. 2008. The mitochondrial permeability transition regulates cytochrome c release for apoptosis during endoplasmic reticulum stress by remodeling the cristae junction. J Biol Chem 283:3476–3486.
Zheng QY, Li PP, Jin FS, Yao C, Zhang GH, Zang T, Ai X. 2013. Ursolic acid induces ER stress response to activate ASK1-JNK signaling and induce apoptosis in human bladder cancer T24 cells. Cell Signal 25:206–213.
Zheng Z, Zhang C, Zhang K. 2010. Role of unfolded protein response in lipogenesis. World J Hepatol 2:203–207.

Supporting Information

Additional supporting information may be found in the online version of this article at the publisher's web-site.